

Chemical and elastic effects on isostructural phase diagrams: The ϵ - G approach

L. G. Ferreira,* A. A. Mbaye,[†] and Alex Zunger
Solar Energy Research Institute, Golden, Colorado 80401
 (Received 9 December 1987)

Numerous theoretical models of temperature-composition phase diagrams of isostructural binary alloys are based on the configurational Ising Hamiltonian in which the many-body configurational interaction energies $\epsilon^{(n)}$ are taken as (volume-independent) constants (the “ ϵ -only” approach). Other approaches postulate phenomenologically composition-dependent but configuration- (σ -) independent elastic energies. We show that under the commonly encountered situation where molar volumes at fixed composition (x) do not depend on the state of order, a new approach is pertinent: We prove that the physically relevant Hamiltonian (the “ ϵ - G approach”) includes the configuration-dependent (but concentration-independent) “chemical” interaction energies $\epsilon^{(n)}$, plus a composition-dependent (but configuration-independent) elastic energy $G(x)$. We compute the elastic term $G(x)$ from the structural and elastic properties of ordered intermetallic systems. We show that inclusion of $G(x)$ into the conventional configurational (ϵ -only) Hamiltonian cures many of the shortcomings of such Ising models in describing actual alloy phase diagrams. In particular, addition of the elastic energy $G(x)$ leads to the following features: (i) narrower single-phase regions and broader mixed-phase regions, (ii) shift of the triple point to substantially higher temperatures, (iii) the mixing enthalpies of the disordered phases become much closer to the experimental data, and (iv) the possibility of the occurrence of metastable long-range-ordered compounds inside the miscibility gap. Cluster-variation and Monte Carlo calculations on model Hamiltonians and on the Cu-Au system are used to illustrate these points.

I. INTRODUCTION

The formation of an ordered compound $A_{M-m}B_m$ ($M = \text{constant}$) from its isostructural constituent elemental solids A and B can be conceptualized to consist of an “elastic” step, where the pure constituent solids $A_{M-m}A_m$ and $B_{M-m}B_m$ are compressed and dilated, respectively, to the cell volume of $A_{M-m}B_m$ through an investment of an elastic energy ΔF , followed by a “flip” of the necessary number of A and B atoms on these prepared lattices $B_{M-m}B_m$ and $A_{M-m}A_m$, respectively (creating thereby $A_{M-m}B_m$), involving a “chemical” (or “substitutional”) energy $\epsilon^{(m)}$. The formation enthalpy $\Delta H^{(m)}$ of $A_{M-m}B_m$ from its constituent solids A and B is then $\Delta F + \epsilon^{(m)}$. Many classical models,¹⁻⁵ constituting the working paradigms of structural chemistry⁶ and metallurgy,¹⁻⁴ have rationalized the stability against dissociation ($\Delta F + \epsilon^{(m)} < 0$) of ordered intermetallic phases by representing the balance between elastic and chemical energies through phenomenological constructs. These include the mismatch between the atomic radii^{2,3} of A and B (used to model the elastic energy), and various scales of electronegativity mismatch³⁻⁵ (modeling the chemical energy). Such are, for example, the model of Darken and Gurry for solid solubilities² (F represented by atomic radii and ϵ by electronegativities), the Miedema model³ for heat of formation (F represented by density mismatch at the Wigner-Seitz cell boundary, ϵ represented by charge transfer), the Mooser-Pearson approach⁷ to phase stability (F represented by the mismatch in valence quantum number, ϵ by the electronegativity), and the orbital radii

method⁸ (F represented by the pseudopotential orbital radius, ϵ by its inverse). In fact, a large body of constructs in metallurgy and structural chemistry^{1,2,6,9,10} has developed around these competing scales, where “elastic factors” are represented by constructs such as “steric hinderance” and the mismatch between various atomic radii, whereas the “chemical effect” is represented by the “electrochemical factor”⁹ and various charge-transfer and electronegativity scales.^{9,10} Numerous examples illustrate the fact that *both* effects are needed, e.g., Laves phases are stabilized *both* by size mismatch and electronegativity differences;¹¹ the existence or nonexistence of certain intermetallic phases has been rationalized by the balance between repulsive elastic and attractive chemical forces.^{3,7,9,10}

It is therefore rather surprising that a whole class of models of alloy phase stability—those¹²⁻¹⁵ that represent the problem of various types of Ising Hamiltonian—have in fact used *constant interaction energies* ϵ , omitting thereby the volume-dependent elastic energy ΔF . These models have a wider scope than the classical models of phase stability: They attempt to predict not only the stable phases but also the transitions between various phases and their coexistence. Indeed, while the temperature-composition phase diagrams of even binary isostructural solids¹⁶ manifest far more diverse phenomena than merely the existence or nonexistence of ordered phases (disordering, miscibility gaps, spinodals, etc.), the complexity associated with the *configurational* degrees of freedom underlying such phenomena has generally limited their modeling to the description of phase interconver-

sion events on a *fixed lattice*, common to A , B , and $A_{M-m}B_m$, i.e., retaining only the volume-independent substitution energies¹²⁻¹⁵ $\{\epsilon^{(m)}\}$. Inspired by the analogous spin- $\frac{1}{2}$ three-dimensional generalized Ising problem,^{12,14} such efforts have generally focused on studies of the properties of this Hamiltonian and on the determination of a set of fixed "chemical energies" $\epsilon^{(m)}$ (analogous to the Ising many-spin interaction parameters) which best describe actual phase phenomena through various approximate solutions of the configurational Hamiltonian, neglecting, however, ΔF .

Whereas the introduction of an ever increasing set of ("multiatom") interaction parameters^{13,17,18} $\{\epsilon^{(m)}\}$, extension of the range of interaction to second and even further neighbors,¹³ and improvements in the methods of solution (Monte-Carlo simulations,^{19,20} high-temperature expansions²¹) have generally resulted in a greater degree of realism, such models often produce but a "caricature of real alloys,"¹⁹ even for the simplest and best studied isostructural face-centered-cubic (fcc) systems. This state of affairs is manifested, among others, by the inability of constant-volume lattice models (see Sec. IV B) to predict from the same Hamiltonian both order-disorder transition temperatures (decided solely by $\epsilon^{(m)}$) and excess thermodynamic energies (e.g., mixing enthalpies, decided primarily by^{22,23} ΔF), the occurrence in pure Ising models for fcc lattices^{19,20} of a triple point at a consistently lower temperature than experiment,¹⁶ the systematic failure to obtain at low temperatures a narrowing of the single-phase regions for ordered structures (instead, the composition domains where ordered compounds exist become *broader* as the temperature is lowered, see Fig. 4(b) below and Sec. IV B), or to predict^{22,23} the appearance of miscibility gaps and ordering in the same phase diagram (observed recently in semiconductors²⁴). Attempts to include elastic energies in Ising-type Hamiltonians²⁵⁻³¹ have emerged recently, but no rigorous formulation of the problem exists.

We will show that these shortcomings reflect primarily the omission of elastic effects—the single most important mechanism of atomic packing in phenomenological models of structural chemistry¹⁻⁸ and in semiconductor alloy phase diagrams.^{22,23} We will demonstrate how chemical and elastic effects can be simply introduced on the same footing in an otherwise purely configurational Hamiltonian under the (most commonly encountered) situation where molar volumes depend only weakly on the state of order. We will then show how most of the qualitative (and in some cases even quantitative) shortcomings of the models which use fixed interaction energies are removed by inclusion of both chemical and elastic energies. This provides a simple method for realistic description of phase phenomena (illustrated here for Cu-Au and semiconductor alloys) within the spirit of generalized Ising models.

II. FORMULATION OF THE PROBLEM: REINTERPRETATION OF COUPLING ENERGIES IN CONFIGURATIONAL HAMILTONIANS

Previous configurational models^{18,19} (either retaining or neglecting elastic effects) assume, at some stage of the

theory, that the lattice parameter of the alloy (or its molar volume) at a given composition does not depend on the state of order (we neglect throughout this paper phonon effects). Often, an even stronger assumption is made—not only is the volume $V(x)$ assumed constant for all phases at a fixed composition x , but the x dependence is also taken to be *linear* (Vegard's rule³²). In what follows we will show that Vegard's rule is much too strong an assumption to be made, in that the deviations from linearity have important *energetic* consequences on phase stability. On the other hand, we explore the full consequences of the assumption that the lattice parameter (and hence molar volumes) is approximately state-of-order independent for fixed composition. We will show that this results in a simple and clear separation of the alloy free energy into chemical (ϵ) and elastic (ΔF) contributions, and that the inclusion of such a new term (ΔF) in the Ising Hamiltonian cures many of its shortcomings in describing alloy phase diagrams. A preliminary brief report on this work has recently appeared.³³

We restrict ourselves to isostructural phase diagrams, i.e., to those binary alloys whose lattice points maintain a one-to-one correspondence to those of the constituent elemental solids at all compositions and structures. We hence bar from consideration those systems that during the alloying process undergo phase transitions to *topologically inequivalent* lattices [e.g., face-centered cubic (fcc) to body-centered cubic (bcc)]. Phase boundaries and phase transformations in such isostructural $A_{M-m}B_m$ binary systems have traditionally been described through lattice models.^{12-15,17-20} There, one considers the 2^N possible arrangements of atoms A and B on a lattice of N points. Each of these will be referred to here as a "state of order" σ (sometimes, also referred to in the literature as a "configuration," or "microstate"). Each arrangement can be characterized by its excess internal energy with respect to equivalent amounts of the pure solids A and B , at their equilibrium molar volumes V_A and V_B , respectively:

$$\Delta E(\sigma, V) = E(\sigma, V) - \frac{N_A}{N} E_A(V_A) - \frac{N_B}{N} E_B(V_B), \quad (2.1)$$

where N_A and N_B are the number of A and B atoms, respectively, in the structure $A_{M-m}B_m$ whose state of order is σ , V is the volume, and E_A and E_B are the volume-dependent total-energy functions of the solids A and B , respectively. On each lattice site i one can have either a B atom (in which case we denote the spin variable as $S^{(i)} = 1$ and the occupation variables as $\eta_1^{(i)} = 1$ and $\eta_0^{(i)} = 0$) or a A atom (in which case the spin variable is $S^{(i)} = -1$ and the occupation variables are $\eta_1^{(i)} = 0$ and $\eta_0^{(i)} = 1$). This general Ising problem is then often simplified^{18,19} by limiting the interaction to a tractable short range and to a finite number of multisite couplings within this range. For instance, limiting the interaction range to first neighbors and truncating the many-atom couplings to include up to four-body terms, the Hamiltonian can be written as¹⁹

$$E = J_0 N + J_1 \sum_{\text{points}} S^{(i)} + J_2 \sum_{\text{pairs}} S^{(i)} S^{(j)} + J_3 \sum_{\text{triangles}} S^{(i)} S^{(j)} S^{(k)} + J_4 \sum_{\text{tetrahedra}} S^{(i)} S^{(j)} S^{(k)} S^{(l)}, \quad (2.2)$$

where the interaction parameters $\{J\}$ can in general be volume dependent. Equivalently, one can use the relations between the spin and the occupation variables

$$\eta_1^{(i)} - \eta_0^{(i)} = S^{(i)} \quad (2.3a)$$

and

$$\eta_1^{(i)} + \eta_0^{(i)} = 1 \quad (2.3b)$$

to express each of the terms in Eq. (2.2) as a sum of products of four occupation variables. For example, the third term in Eq. (2.2) can be written as

$$\sum (\eta_1^{(i)} - \eta_0^{(i)}) (\eta_1^{(j)} - \eta_0^{(j)}) (\eta_1^{(k)} + \eta_0^{(k)}) (\eta_1^{(l)} + \eta_0^{(l)}).$$

The Hamiltonian of Eq. (2.2) can hence also be written in the form

$$E = \sum_{p,q,r,s=0,1} E(p,q,r,s) \frac{1}{N_4} \sum_t \eta_p^{(i)} \eta_q^{(j)} \eta_r^{(k)} \eta_s^{(l)} \quad (2.4)$$

(where t denotes tetrahedra and N_4 is their number). Applying the transformation implied by Eq. (2.1), defining the multiple index $n = (p, q, r, s)$ which identifies the arrangement of A and B on a tetrahedron, and expressing the state-of-order-dependent multisite correlation functions as

$$\xi_n(\sigma) = \frac{1}{N_4} \sum_t \eta_p^{(i)} \eta_q^{(j)} \eta_r^{(k)} \eta_s^{(l)}, \quad (2.5)$$

Eqs. (2.1) and (2.4) become

$$\Delta E(\sigma, V) = \sum_n \Delta E(n, V) \xi_n(\sigma). \quad (2.6)$$

The multisite correlation functions $\xi_n(\sigma)$ can be thought of as occurrence frequencies, in the sense that by Eq. (2.5) they are positive and normalized

$$\sum_n \xi_n(\sigma) = 1.$$

In a system with a given distribution σ of atoms, $\xi_n(\sigma)$ is the frequency with which the basic cluster (tetrahedron, in the present case) appears with occupation $n = (p, q, r, s)$, i.e., the frequency of tetrahedra having occupation p in the vertex belonging to the first sublattice, q in the vertex of the second, etc. Therefore, given the state of order σ , $\{\xi_n\}$ are determined by counting tetrahedra, as implied by the definition of Eq. (2.5). Clearly, $\xi_n(\sigma)$ are functions of the state of order. On the other hand, given a set of positive and normalized frequencies $\{\xi_n(\sigma)\}$, there are infinitely many states of order belonging to this set. For instance, one can break the crystal into macroscopic domains of pure ordered compounds, (i.e., regions whose clusters have just one type of occupation n), and choose the size and number of the domains to match the given set of frequencies $\{\xi_n\}$. (The

clusters at the domain boundaries are negligible if the domains are macroscopic.) Thus, although the ξ_n are functions of σ , the state of order σ itself is not a function of the finite set of ξ_n .

The reduction of the Hamiltonian Eq. (2.2) to the form¹⁹ of Eq. (2.6), can be simply illustrated in the case of fcc alloys. If N is the number of lattice points, there are $6N$ first-neighbor pairs, $8N$ triangles, and $2N$ tetrahedra. Thus, the energy parameters $E(p, q, r, s)$ of Eq. (2.4) (where the indices denote the number of A atoms—1 or 0—on the respective tetrahedron sites) are

$$\begin{aligned} E(0,0,0,0) &= J_0 N - J_1 N + 6J_2 N - 8J_3 N + 2J_4 N, \\ E(1,0,0,0) &= J_0 N - \frac{J_1 N}{2} + 0 + 4J_3 N - 2J_4 N, \\ E(1,1,0,0) &= J_0 N + 0 - 2J_2 N + 0 + 2J_4 N, \\ E(1,1,1,0) &= J_0 N + \frac{J_1 N}{2} + 0 - 4J_3 N - 2J_4 N, \\ E(1,1,1,1) &= J_0 N + J_1 N + 6J_2 N + 8J_3 N + 2J_4 N, \end{aligned} \quad (2.7)$$

[recall that for an A -only atomic arrangement, all S values of Eq. (2.2) are -1]. In the unlikely case where at all compositions x the alloy has the same equilibrium lattice parameter and molar volume, the excess energy relative to equivalent amounts of pure A and B at their equilibrium can be written as

$$\begin{aligned} \varepsilon^{(0)} &\equiv \Delta E(0,0,0,0) = 0, \\ \varepsilon^{(1)} &\equiv \Delta E(1,0,0,0) = -6J_2 N + 8J_3 N - 4J_4 N, \\ \varepsilon^{(2)} &\equiv \Delta E(1,1,0,0) = -8J_2 N, \\ \varepsilon^{(3)} &\equiv \Delta E(1,1,1,0) = -6J_2 N - 8J_3 N - 4J_4 N, \\ \varepsilon^{(4)} &\equiv \Delta E(1,1,1,1) = 0, \end{aligned} \quad (2.8)$$

where N is the total number of lattice points. Indeed, many lattice models of alloys have adopted this viewpoint,^{18,19} solving approximately the thermodynamics for a Hamiltonian of Eq. (2.6) with the constant interaction parameters $\varepsilon^{(n)}$ of Eq. (2.8).

In general, however, the lattice parameter (hence volume) changes with composition.¹⁶ Hence, each of the interaction "parameters" $\Delta E(n, V)$ of Eqs. (2.6)–(2.8) is, in fact, volume dependent (i.e., an "equation of state" at $T=0$). The physical content of these volume-dependent parameters $\Delta E(n, V)$ can be conceptualized in the following way. If all the N_4 tetrahedra have the same occupation numbers n (in which case one has an ordered crystal with a configuration of the basic cluster and a state of order denoted as $\sigma = n$) then Eq. (2.5) implies that the multisite correlations are

$$\xi_m(n) = \delta_{nm}. \quad (2.9)$$

Conceptualizing such a state of order as a periodic crystal whose configuration is the basic cluster (a tetrahedron), Eq. (2.6) lets us interpret the volume-dependent parameters $\Delta E(n, V)$ as the excess energy of the ordered structure n . An alloy could then be described as a collection of all local atomic environments exhibited by all such or-

dered crystals, where each local arrangement occurs in the alloy with the frequency $\xi_n(\sigma)$. Thus, at *any* state of order σ of the system (ordered or not), the equilibrium volume $V_{\text{eq}}(x)$ is given by the minimum condition

$$\frac{d}{dV} \Delta E(\sigma, V) = \sum_n \xi_n(\sigma) \frac{d}{dV} \Delta E(n, V) = 0, \quad (2.10)$$

whereas the bulk modulus of the system would be

$$\begin{aligned} B(\sigma, V) &= V \frac{d^2}{dV^2} \Delta E(\sigma, V) = \sum_n \xi_n(\sigma) V \frac{d^2}{dV^2} \Delta E(n, V) \\ &= \sum_n \xi_n(\sigma) B(n, V), \end{aligned} \quad (2.11)$$

i.e., a combination of the bulk moduli $B(n, V)$ of the corresponding ordered structures.

Considering a (canonical) ensemble of samples of given concentration x , the probability of finding a given ordered structure becomes a thermal average

$$P_n(x, T) = \langle \xi_n(\sigma) \rangle, \quad (2.12)$$

and the excess enthalpy of mixing¹⁶ at the equilibrium volume V_{eq} becomes

$$\Delta H(x, T) = \sum_n \Delta E(n, V_{\text{eq}}) P_n(x, T). \quad (2.13)$$

The thermal average Eq. (2.12) is also used in Eqs. (2.10) and (2.11) to determine the equilibrium volume and bulk modulus. In general, these will be both concentration and temperature dependent.

Numerous authors¹⁷⁻²⁰ have replaced $\Delta E(n, V)$ by the *volume-independent* excess energies $\Delta E(n)$. This would suggest by Eq. (2.11) that the alloy has a vanishing bulk modulus. In fact, numerous measurements³⁴ support the notion that the bulk modulus of many alloys is of the *same order of magnitude* (with minor nonlinearities) as that of its constituents. We will show below (Sec. IV) that the replacement of the conventional volume-independent interaction energies $\Delta E(n)$ by $\Delta E(n, V)$ is also required to obtain the correct order of magnitude of the excess enthalpy of mixing $\Delta H(x, T)$ of Eq. (2.13).

III. SEPARATION OF ELASTIC AND CHEMICAL EFFECTS IN $\Delta E(\sigma, V)$.

Given the fact that the interaction energies $\Delta E(n, V)$ of Eq. (2.6) are generally functions of volume rather than constants, we now isolate the two physical factors contributing to it: the “elastic” (n -independent but V -dependent) and the “chemical” (constant-volume but n -dependent) contributions.

A. Simple conceptual model

The content of $\Delta E(n, V)$ of Eq. (2.6) can be first appreciated *qualitatively* by considering the formation of a perfectly ordered crystal $A_{M-m}B_m$ (generated by repeating the M -atom cluster $A_{M-m}B_m$, hence $\sigma \equiv m$) with N_A atoms A and N_B atoms B from the constituent solids A and B , in two formal steps (a mathematical derivation follows in the next section). *First*, compress or dilate the

pure crystal $A_{M-m}A_m$ from its equilibrium structure with molar volume V_A to the molar volume V appropriate to the final structure of $A_{M-m}B_m$. Do the same for the pure crystal $B_{M-m}B_m$, changing it from the volume V_B to V . Since a deformation of the equilibrium structures of A and B is involved in this step, it requires an *investment* of elastic energy. For a compound $A_{M-m}B_m$ at a volume V , this energy investment is simply

$$\begin{aligned} \Delta F[N_A, N_B; V] &= \frac{N_A}{N} (E[A; V] - E[A; V_A]) \\ &+ \frac{N_B}{N} (E[B; V] - E[B; V_B]). \end{aligned} \quad (3.1)$$

Second, convert (i.e., “flip”) the necessary number of A atoms in $A_{M-m}A_m$ into B (and vice versa for $B_{M-m}B_m$) on these “prepared” fixed lattices with volume V . If there exists in addition, a *common* sublattice C (e.g., as in $AC+BC$ zinc-blende alloys), relax this sublattice (keeping A and B fixed) to achieve minimum energy. This second step in our procedure involves the “spin-flip” or “chemical” energy $\epsilon^{(m)}$ associated with interactions between A and B (e.g., charge transfer, polarization, hybridization, spin-spin coupling) on a *fixed* A - B lattice. (We use throughout this paper the term “elastic energy” to denote energy changes associated with *volume* changes of the A - B sublattice. “Chemical energy” will denote energy change at constant volume of the primary A - B sublattice, including, however, volume-preserving geometry changes in the common sublattice, if it exists.) The fixed-volume chemical energy ϵ is the only contribution included in conventional lattice models of phase diagrams.¹⁷⁻²⁰ $\epsilon^{(m)}$ could be either positive or negative. We define its value at the equilibrium volume V_m of the ordered crystal consisting only of $A_{M-m}B_m$ tetrahedra as

$$\begin{aligned} \epsilon^{(m)} &= E[A_{M-m}B_m; V_m] - \frac{N_A}{N} E[A; V_m] \\ &- \frac{N_B}{N} E[B; V_m]. \end{aligned} \quad (3.2)$$

As in Eq. (2.8), $\epsilon^{(m)}$ is the excess energy of the structure $A_{M-m}B_m$, at its equilibrium volume V_m , with respect to the energies of equivalent amounts of its constituents, also at V_m . Note again that if a common sublattice C exists, the first term on the right-hand side of Eq. (3.2) corresponds to the total energy after sublattice C is relaxed to the energy-minimizing configuration, hence, $\epsilon^{(m)}$ incorporates automatically such cell-internal relaxation. Clearly the sum of Eqs. (3.1) and (3.2)

$$\Delta E(m, V) = \Delta F[N_A, N_B; V] + \epsilon^{(m)} \quad (3.3)$$

gives the total excess energy of the perfectly ordered structure consisting of $A_{M-m}B_m$ units as a function of its volume. We will assume that this corresponds to the energies $\Delta E(m, V)$ summed over in Eq. (2.6). The enthalpy of formation of this ordered phase from the elemental solids A and B is given by the equilibrium value [$d\Delta E(m, V)/dV=0$, where $V=V_m$] of $\Delta E(m, V)$, i.e.,

$$\Delta H^{(m)} = \Delta F[N_A, N_B; V_m] + \epsilon^{(m)}. \quad (3.4)$$

Such an ordered phase is said to be "stable against disproportionation into its constituents" ($\Delta H^{(m)} < 0$) if its negative chemical energy $\varepsilon^{(m)}$ overwhelms the positive elastic energy at equilibrium $\Delta F[N_A, N_B; V_m]$ invested in deforming its constituents; otherwise this phase is "unstable towards disproportionation."³⁵

Using Eqs. (2.13) and (3.3), we can now describe the mixing enthalpy of a *disordered* (D) alloy which exhibits all local atomic environment characteristics of all ordered arrangements $\{n\}$ as

$$\Delta H^{(D)}(x, T) = \sum_n P_n(x, T) \varepsilon^{(n)} + \tilde{G}(x, T), \quad (3.5)$$

where, from Eq. (3.3) and (2.13) the average elastic energy of the alloy is

$$\tilde{G}(x, T) = \sum_n P_n(x, T) \Delta F[N_A, N_B; V(x)] \quad (3.6)$$

and $V(x)$ is the alloy equilibrium volume satisfying $d\tilde{G}(x)/dV=0$. The general decomposition of Eqs. (3.3)–(3.6) illustrates the interplay between positive-definite elastic energies $\tilde{G}(x, T)$ and the chemical energies $\varepsilon^{(n)}$, and the possibility^{22,23} that $\Delta E(n, V)$ [or equivalently, J_n of Eq. (2.7)] can *change sign* as a function of volume.

In what follows we will prove that when molar volumes are state-of-order independent for fixed compositions, the form of Eq. (3.5) can be derived rigorously, and that under these conditions $\tilde{G}(x, T)$ is reduced to a *temperature-independent* and readily calculable function $G(x)$. Its effect on the phase diagrams will be discussed in Sec. IV, and the consequences of this interplay will be discussed in Secs. V–VII.

B. Conditions and exact form of $\Delta E(\sigma, V)$.

It is possible to derive a general expression for the elastic energy $G(x)$ of an alloy in terms of simple measurable quantities if one assumes that the *equilibrium molar volume depends on composition but not on the state of order* (the trivial effect of thermal expansion of the volume is not included here, but can be easily incorporated in the results below). This assumption is the traditional cornerstone of structural chemistry,^{5,6} where an even stronger statement is made: Each atom can be characterized by a radius (atomic, metallic, covalent, van der Waals, etc.), approximately independent of its chemical environment. This assumption seems to be supported by numerous experimental observations,³⁴ some examples are compiled in Table I. In practice we can accept small volume changes from V_0 to V_1 attendant upon a phase transition, as long as the change in elastic energy $\frac{1}{2}BV_0[(V_1 - V_0)/V_0]^2$ needed to bring V_1 back to V_0 is small compared with the energy terms determining the phase diagram. For example, in an order-disorder transition at room temperature (T_0) the entropy contribution to the free energy changes by approximately $RT_0 \ln 2 = 0.42$ kcal/mol. Thus, if $\frac{1}{2}BV_0[(V_1 - V_0)/V_0]^2$ is smaller than about 0.1 kcal/mol, the molar volume change $V_1 - V_0$ can be neglected. In Table I we list the molar volumes for some noble-metal-containing alloys with different structures.

(The case of the noble metals was chosen because they have high values of the product BV , and therefore significant elastic effects.) For example, for metallic gold one has³⁴

$$\frac{1}{2}BV = 0.211 \text{ kcal/mol}.$$

Thus, in Table I it is sufficient to verify that the volume changes following the changes in structure are such that

$$\left| \frac{V_1 - V_0}{V_0} \right| \leq 2.2\%.$$

This is indeed satisfied by the data (Table I). Note that if the molar volume had changed considerably with the state of order σ , then in the disordered phase it would vary from one sample to another even at a fixed composition. This, however, is generally not observed. Note further that, in general, our requirement of state-of-order independence of volumes applies only to those "sample" states that are used to represent the system in an "interesting" temperature interval. For example, a Monte Carlo calculation on a 1000-spin system involves in principle $2^{1000} = 10^{301}$ states, but only a far smaller number of "representative" spin configurations^{19,20} (say, $10^6 - 10^8$), are typically computed. Only this subset of states is needed to fulfill our requirement of state-of-order-independent volumes.

Assuming state-of-order independence of molar volumes at fixed compositions, we prove in Appendix I that $\Delta E(\sigma, V)$ of Eq. (2.6) assumes the simple form

$$\Delta E(\sigma, V) = \sum_n \xi_n(\sigma) \varepsilon^{(n)} + g(x, V), \quad (3.7)$$

where $\varepsilon^{(n)}$ are the volume-independent chemical or "ordering" energies of Eq. (3.2), and $g(x, V)$ is given for the composition x and at any volume, (even outside equilibrium) by

$$\begin{aligned} g(x, V) = & \int_{V_A}^V X(V') \frac{B(V')}{V'} \frac{dV'}{dX} dV' \\ & - x \int_{V_B}^V \frac{B(V')}{V'} \frac{dV'}{dX} dV' \\ & - x \int_{V_A}^{V_B} X(V') \frac{B(V')}{V'} \frac{dV'}{dX} dV'. \end{aligned} \quad (3.8)$$

Here, $X(V)$ is the equilibrium concentration when the volume is V , $B(V)$ is the bulk modulus at equilibrium when the volume is V , and as used before, V_A and V_B are the equilibrium molar volumes for the pure solids A and B , respectively. One readily verifies that at equilibrium, [namely, when $x = X(V)$], Eq. (2.10) holds.

To obtain an expression for $g(x, V)$ at equilibrium, we integrate on X in Eq. (3.8) instead of on V and choose $V = V(x)$ to be the *equilibrium* volume for a given composition x . Then, Eq. (2.6) becomes

$$\Delta E(\sigma) \equiv \Delta E(\sigma, V) = \sum_n \xi_n(\sigma) \varepsilon^{(n)} + G(x), \quad (3.9)$$

where $V = V(x)$ and where for

$$Z(X) = \frac{B(X)}{V(X)} \left[\frac{dV}{dX} \right]^2$$

TABLE I. Data (Ref. 34) on molar volumes of intermetallic phases at room temperature showing that for fixed stoichiometry the volume depends only weakly on the type of order.

Formula	Space group (type or phase)	Molecular volume (Å ³)	Formula	Space group (type or phase)	Molecular volume (Å ³)
AgCd	<i>Pm 3m</i>	36.97	AuLi	<i>Pm 3m</i>	29.73
	<i>P6₃/mmc</i>	37.28		tetragonal	29.53
	<i>Im 3m</i>	36.76		orthorombic	29.66
Ag ₃ Pt	<i>Fm 3m</i>	59.37	Au ₃ Mn	orthorombic	66.73
	<i>Pm 3m</i>	59.09		tetragonal	66.41
AgPt ₃	<i>Pm 3m</i> (γ)	59.32	AuMn	<i>I4/mmm</i>	32.44
	cubic (γ')	60.24		orthorombic	32.95
Ag ₂ S	<i>P2₁/n</i>	56.71	AuNb ₃	<i>Pm 3m</i>	70.30
	<i>Im 3m</i>	57.57		<i>Im 3m</i>	70.58
Ag ₂ Se	<i>P222₁</i>	59.91	AuTe ₂	<i>C2/m</i>	80.54
	tetragonal	59.27		<i>Pma</i>	81.33
AgTe	<i>P4/mmm</i> (AuCu)	34.33	AuTi	<i>Pmma</i>	33.26
	<i>P4/mmm</i> (TiCu)	34.23		<i>P4/nmm</i>	33.52
AgZn	<i>Im 3m</i>	31.44	AuV ₃	<i>Pm 3n</i>	57.96
	<i>Pm 3m</i>	31.43		<i>Im 3m</i>	57.87
AsCu ₃	<i>I43d</i>	55.49	Au ₃ Zn	<i>Abam</i>	65.02
	tetragonal	56.09		<i>I4₁/acd</i>	65.14
Au ₃ Be	orthorombic	58.73	Au ₅ Zn ₃	<i>Ibam</i>	255.2
	tetragonal	57.75		<i>Pmc2₁</i>	255.1
Au ₃ Cd	tetragonal	70.05	CuBe	<i>Pm 3m</i>	19.75
	<i>P6₃/mmc</i>	70.09		tetragonal	19.77
AuCd	<i>Pm 3m</i>	36.82	Cu ₄ Cd ₃	<i>P4₂/ncm</i>	15.56
	<i>Pmma</i>	36.62		<i>F43m</i>	15.41
AuCu	<i>Fm 3m</i>	58.23	Cu ₃ Ge	<i>P2₁</i>	50.48
	<i>P4/mmm</i>	57.78		<i>Pmnm</i>	50.58
Au ₇ Ga	<i>Fm 3m</i>	67.52	Cu ₃ Ti ₂	<i>I4/mmm</i>	68.83
	<i>P6₃/mmc</i>	67.43		<i>P4/nmm</i>	68.33
Au ₈ In	<i>Fm 3m</i>	69.50	CuZn	<i>Im 3m</i>	25.70
	<i>P6₃/mmc</i>	69.62		<i>Pm 3m</i>	25.65
Au ₃ Li	<i>Pm 3m</i>	62.61			
	tetragonal	63.04			

one has

$$G(x) = (1-x) \int_0^x XZ(X) dX + x \int_x^1 (1-X)Z(X) dX . \quad (3.10)$$

In many practical applications, $G(x)$ could be simplified (if needed) by noting that it is always non-negative, vanishes, by definition, at the end-point compositions $x=0$ and $x=1$, and has a negative second derivative

$$\frac{d^2G(x)}{dx^2} = -Z(x) . \quad (3.11)$$

Hence, if one wishes, $G(x)$ could be approximated by a simple function with the same properties

$$G(x) \simeq \Omega x(1-x) , \quad (3.12)$$

and define the "effective elastic interaction parameter" Ω by equating the areas under the curves

$$\Omega \int_0^1 x(1-x) dx = \int_0^1 G(x) dx, \quad (3.13)$$

or

$$\Omega = 3 \int_0^1 x(1-x) Z(x) dx. \quad (3.14)$$

Equations (3.9) and (3.10) are our central results and determine the thermodynamic behavior of the alloy. They have the following simple interpretation: The first term on the right-hand side of Eq. (3.9) represents the energy of an alloy whose volume V equals that of its constituents (V_A and V_B), i.e., for the uncommon case of a lattice-matched alloy or one that has a vanishing bulk modulus. The configuration-dependent (but volume- and composition-independent) chemical energies $\epsilon^{(n)}$ are simply related to the familiar Ising-type spin-flip substitution energies on this fixed lattice [e.g., Eq. (2.8)]. They measure the strength of the many-body interactions between atoms (or spins) within the interaction range considered. The only reason that the first term of Eq. (3.9) changes with composition is *statistical*: Different alloy compositions have different distributions of species n , [given by $\xi_n(\sigma)$], but $\epsilon^{(n)}$ itself is fundamentally composition independent.

The second, new term of Eq. (3.9) represents corrections to the constant-volume assumption. It vanishes by Eq. (3.10) [or (3.14)] when the alloy has the same volume as its constituents, i.e., when $dV/dx=0$, or, equivalently, when the alloy is infinitely compressible [$B(V)=0$]. The two terms in Eq. (3.9) reflect the dual coordinates used in phenomenological models of solid solubility, compound stability, and mixing enthalpies: The second term can be thought to describe the destabilizing effect of strain induced by the mismatch between the molar volumes of the constituents, and parallels the classical "size factor" in alloy models,¹⁻⁴ whereas the first term can be thought to qualitatively describe the "electronegativity factor" of Darken and Gurry,² Miedema,³ and Pauling,⁵ and reflects the effect of chemically specific interactions.

The existence of the new $G(x)$ term in the otherwise purely configurational alloy Hamiltonian has a few obvious consequences.

(i) Equation (3.4) demonstrates that the constant energies $\epsilon^{(n)}$ appearing in Ising Hamiltonians [e.g., Eq. (2.8)] are *not* the enthalpies of formation of the ordered phases n . Hence, the nonexistence of an ordered compound ($\Delta H^{(n)} > 0$) does not testify to the fact that the fundamental atom-atom interactions $\epsilon^{(n)}$ are positive. This is evident if one considers the pure solids A ($x=0$) and B ($x=1$) and observes that $G(0)=G(1)=0$ by Eq. (3.10). Setting the reference energies as before [Eq. (2.8)] to $\epsilon^{(AA)}=\epsilon^{(BB)}=0$, the enthalpy of formation $\Delta H^{(n)}$ of a perfectly ordered structure [Eq. (3.4)] is simply the energy $\Delta E(\sigma)$ specialized to this state of (perfect) order $\sigma=n$. In this case ($x=X_n$) we have $\xi_m(n)=\delta_{nm}$, or $\Delta E(n)=\Delta H^{(n)}$. From Eq. (3.9) one hence obtains

$$\epsilon^{(n)} = \Delta H^{(n)} - G(X_n). \quad (3.15)$$

This simple result reveals the tacit relation between thermodynamic energies (e.g., $\Delta H^{(n)}$) and critical temperatures: Since order-disorder transformations occurring at a

fixed composition X_n are not affected by $G(X_n)$ [a term which is common in Eq. (3.9) to both the ordered and the disordered phases at $x=X_n$], the specification of $\epsilon^{(n)}$ suffices to determine such order-disorder transition temperatures.¹⁷⁻²⁰ However, thermodynamic excess energies are determined [by Eqs. (2.13) and (3.9)] *both* by chemical ($\epsilon^{(n)}$) and elastic [$G(x)$] energies.^{22,23} Hence, failing to incorporate $G(x)$ in the Hamiltonian would result in erroneous thermodynamic energies in lattice-mismatched systems. Conversely, erroneous transition temperatures would result if the energy parameters $\epsilon^{(n)}$ are identified with the (measured or calculated) formation enthalpies $\Delta H^{(n)}$ of the corresponding ordered phases. This will be illustrated in Sec. IV.

(ii) since $G(x)$ depends on an integral of $(dV/dX)^2$ [Eq. (3.10)], the often-neglected small deviations from Vegard's rule (which states that $dV/dx=\text{const}$) may significantly affect $G(x)$. This is illustrated in Sec. IV.

(iii) As stated above, if one is interested in fixed-composition phase transformations (e.g., antiferromagnetic to disordered), $G(x)$ is unimportant. In contrast, phase separation, spinodal decomposition or any other *many-phase coexistence phenomena* are affected by $G(x)$. This is obvious if one considers an example where x_1 and x_2 are the compositions of two phases in equilibrium. By assumption, $x_1 \neq x_2$. Now switch on $G(x)$ in Eq. (3.9). Since in general $G(x_1) \neq G(x_2)$, the two phases cannot be in equilibrium any longer. Their equilibrium compositions would have to be shifted to x'_1 and x'_2 , thus altering the shape of the phase diagram. This is illustrated in Sec. IV (and Fig. 4 below).

C. Comparison with previous approaches

Equations (3.9)–(3.15) can serve to illustrate many of the various approaches adopted in the past to the alloy phase diagram problem.

First, contemporary models of semiconductor phase diagrams³⁶⁻³⁹ have generally ignored the n -dependent chemical energies, retaining various approximations to the elastic energy $G(x)$ alone. This "G-only" approach precludes the existence of any ordered intermediate phases or order-disorder transformations, in agreement with the then-available data, but in apparent conflict with recent observations.²⁴ These approaches include the "ideal solution model",^{36,39} [$\epsilon^{(n)}=0$; $G(x)=0$], the "regular solution model",³⁷ [$\epsilon^{(n)}$ pairwise additive, and $G(x)=0$], and the elastic model of Fedders and Muller.³¹ These approaches correctly predict the order of magnitudes and trends in the observed interaction parameter $\Omega \equiv \Delta H^{(D)}(x)/x(1-x)$ in semiconductors [where $\Delta H^{(D)}$ is given by Eq. (3.5)], but fail to exhibit its (x, T) dependence,³⁸ or the strong departure of the probabilities $P_n(x, T)$ of Eq. (3.5) from a *random* distribution (an effect often termed as "clustering"). Furthermore, these approaches characterize elastic interactions [proportional to the square of the lattice parameter or atomic radii mismatch $\Delta a^2=(a_A-a_B)^2$] as always destabilizing, in conflict with numerous classical counterexamples (e.g., Laves phases can be *stabilized*¹¹ by large Δa 's).

Second, a large class of models addressing *coherent*

phase diagrams on a fixed lattice^{12-15,17-20} (that common to A , B , and $A_{1-x}B_x$) have naturally ignored the elastic energy $G(x)$. While these models have provided a wealth of information on the generic structure of the phase diagram in terms of the signs and magnitudes of the $\epsilon^{(n)}$'s, a number of shortcomings in representing actual phase phenomena have been noted.^{12-15,17-20} Specifically, the application of this pure Ising (" ϵ -only") approach to actual phase diagrams has three significant consequences. (i) Since the choice of the sign of the interaction energies $\epsilon^{(n)}$ in simple Ising models uniquely determines whether the system is of the ferromagnetic, separating type ($\epsilon^{(n)} > 0$), or of the antiferromagnetic, ordering type ($\epsilon^{(n)} < 0$), the two behaviors are generally mutually exclusive (unless an unmotivated mix of positive and negative ϵ 's is postulated). This conflicts with the often observed coexistence of miscibility gaps and order-disorder transformations in the same phase diagram.²⁴ (ii) In tacitly identifying $\epsilon^{(n)}$ with the enthalpy of formation $\Delta H^{(n)}$ of the ordered phase [which is the case in the absence of any other interaction; see Eq. (3.15)], it became impossible to reconcile the observed transition temperatures with thermodynamic data. For example, adjusting¹⁸ $\epsilon^{(2)}$ of the Cu-Au system to the observed order-disorder critical temperature at $x = \frac{1}{2}$ one obtains $\epsilon^{(2)} = -5.3$ kcal, in substantial disagreement with $\epsilon^{(2)} \equiv \Delta H^{(2)} = -2.1$ kcal measured directly.¹⁶ Furthermore, in an attempt to explain the near immiscibility^{16(a)} of Cu and Ag, positive values of $\epsilon^{(n)}$ were taken,¹⁸ whereas first-principles total-energy calculations³³ show $\epsilon^{(n)} < 0$ [but $G(x) > 0$, so $\Delta H^{(n)} > 0$]. (iii) These approaches require that if $\Delta H^{(D)} > 0$ (as is the case for all semiconductor alloys^{36,37}) no ordering can exist, and conversely, if ordering exists, one must have $\Delta H^{(D)} < 0$, both in conflict with the data.^{16,24,36}

In what follows we build on the experience gained in previous work on the ϵ -only Ising model, and show how its predictions can be improved both qualitatively and quantitatively by adding a simple, physically motivated, and readily derivable term $G(x)$, to the Hamiltonian.

Equations (3.9) and (3.10) can be used as input to a phase-diagram calculation [i.e., solving for $\xi_n(\sigma)$ in Eq. (3.9) for all phases, as a function of x and T] if $\{\epsilon^{(n)}\}$ and $B(x)$, $V(x)$ are known. In the absence of continuous data for B and V as a function of x , these might be approximated by interpolating the data from a few ordered structures²²ⁿ. For example, one could perform first-principles total energy calculations on a set of ordered structures A_nB_m [with stoichiometric compositions $X_n = m/(n+m)$ and $1-X_n = n/(n+m)$] that are likely to become the ground states⁴⁰ of the $A_{1-x}B_x$ system. From such calculations^{22,23} one routinely obtains for ordered crystals the equation of state $\Delta E(n, V)$ of Eq. (2.1), the equilibrium volumes V_n , the bulk moduli B_n , and the equilibrium values of $\Delta E(n, V_n) \equiv \Delta H^{(n)}$. One can then compute $G(x)$ of Eq. (3.10) by the following process: (i) Interpolate $\{B_n\}$ to obtain $B(x)$; (ii) interpolate $\{V_n\}$ to obtain $V(x)$; (iii) using $B(x)$ and $V(x)$, integrate Eq. (3.10) to obtain $G(x)$; and (iv) given this $G(x)$, evaluate its magnitude $G(X_n)$ at the stoichiometric compositions X_n . (v) Use Eq. (3.15) and the calculated $\{\Delta H^{(n)}\}$ (for fully relaxed ordered structures) to find $\{\epsilon^{(n)}\}$. These

$G(x)$ and $\epsilon^{(n)}$ can then be used to solve for $\xi_n(\sigma)$ in Eq. (3.9) by any of the statistical mechanics methods available (Monte Carlo,¹⁹ the cluster variation method⁴¹), to obtain both the full phase diagram and the thermodynamic functions [e.g., $\Delta H(x, T)$ in Eq. (2.13)]. The extent of agreement or disagreement obtained with the observed phase diagram can be used to judge the underlying assumption of transferability of ordered phase data to the alloy environment. This program has been carried out for the Cu-Au system, and the results were reported elsewhere.⁴²

Alternatively, one can reverse the procedure and find $G(x)$ and $\{\epsilon^{(n)}\}$ underlying the experimental data itself. This is possible if sufficient data exists for $\{B_n, V_n, \Delta H^{(n)}\}$ of the ordered phases. From this structural and thermodynamic data one could then repeat steps (i)–(v) above and predict the phase diagram. In what follows we adopt this approach and illustrate the method for the Cu-Au system, for which reasonably sufficient experimental data exist.

We will illustrate the method in two ways. First (Sec. IV A) we will use the experimental data $\{B_n, V_n, \Delta H^{(n)}\}$ for the ordered structures $\text{Cu}_{4-n}\text{Au}_n$ and calculate from these $G(x)$ and $\{\epsilon^{(n)}\}$. Solving (approximately) for the $\xi_n(\sigma)$ of Eq. (3.9) will then give the predicted order-disorder transition temperatures, to be compared with experiment. This will establish the extent to which elastic and thermodynamic data on five ($0 \leq n \leq 4$) ordered structures alone can be used in our formalism to predict critical data throughout the temperature and composition ranges. Second (Sec. IV B), we will adjust our $\{\epsilon^{(n)}, G(x)\}$ to fit precisely the known critical data, and contrast the phase diagram obtained with ϵ only to that obtained with both ϵ and G . This will establish the role of elastic energies on the form of the phase diagram.

IV. RESULTS

A. Predicting critical temperatures of the Cu-Au system from thermodynamic data alone

We now apply the ϵ - G formalism to calculate the phase diagram of the Cu-Au system in the tetrahedron approximation, where $0 \leq n \leq 4$ denotes the five possible $\text{Cu}_{4-n}\text{Au}_n$ tetrahedra, as well as the unit cells of the five corresponding ordered crystals.

Table II summarizes the observed data on $\{B_n, V_n, \Delta H^{(n)}\}$ for the ordered $\text{Cu}_{4-n}\text{Au}_n$ phases.^{16,34} Since our method works best when the volume at a given composition has but a small dependence on the state of order, we need to select V_n that best satisfies this condition. No problem exists for ordered CuAu-I whose molar volumes (or lattice parameter) change little on the order-disorder transformation (see Sec. III). However, Cu_3Au does exhibit a non-negligible change of volume⁴³ as the temperature is raised above the order-disorder transition temperature (663 K) for $x=0.25$. For an optimal description of the order-disorder transformation we hence choose the room-temperature molar volume of disordered samples prepared just above the transition temperature. The case of CuAu_3 is even less clear. There, the state of order corresponding to the molar

volume quoted Table II is uncertain,⁴⁴ and even the enthalpy of formation $\Delta H^{(3)}$ is not known. We hence disregard B_3 and V_3 , and interpolate the remaining B_n 's and V_n 's, for $n=0,1,2,4$ with third-order polynomials, to obtain $B(x)$ and $V(x)$ (other functional forms for the interpolation could change the results somewhat). Integrating Eq. (3.14) with these $B(x)$ and $V(x)$ to obtain the approximation (3.12), one then finds the function $G(x)$ depicted in Fig. 1 by solid circles. The corresponding $dV(x)/dx$ function is shown by the solid circles in Fig. 2, and exhibits substantial deviations from Vegard's rule (dashed line in Fig. 2). Correspondingly large deviations are noted in $G(x)$ if Vegard's rule is used (dashed line in Fig. 1). The calculated chemical energies $\epsilon^{(n)}$ obtained from Eq. (3.15) using the $\Delta H^{(n)}$ values of Table II and $G(X_n)$ of the dotted curve in Fig. 1 (defining again $\epsilon^{(0)} = \epsilon^{(4)} = 0$) are

$$\begin{aligned}\epsilon^{(1)} &= -4.607 \text{ kcal/mol}, \\ \epsilon^{(2)} &= -5.963 \text{ kcal/mol}, \\ \epsilon^{(3)} &= -4.267 \text{ kcal/mol},\end{aligned}\quad (4.1)$$

and the elastic energies at equilibrium (from Fig. 1) are

$$\begin{aligned}G(X_1) &= 2.897 \text{ kcal/mol}, \\ G(X_2) &= 3.863 \text{ kcal/mol}.\end{aligned}\quad (4.2)$$

The formation enthalpies of the ordered phases are given by Eq. (3.15) as the sum of Eqs. (4.1) and (4.2), i.e.,

$$\begin{aligned}\Delta H^{(1)} &= -1.71 \text{ kcal/mol}, \\ \Delta H^{(2)} &= -2.10 \text{ kcal/mol},\end{aligned}\quad (4.3)$$

as given in Table II. Clearly, the elastic energies at equilibrium [Eq. (4.2)] are significant relative to the chemical energies [Eq. (4.1)].

The transition temperatures T_1 and T_2 for order-disorder transformation for $\text{Cu}_3\text{Au} \rightleftharpoons \text{Cu}_{0.75}\text{Au}_{0.25}$ and $\text{CuAu} \rightleftharpoons \text{Cu}_{0.5}\text{Au}_{0.5}$, respectively, depend, as discussed above, on the $\epsilon^{(n)}$'s but not on $G(x)$. Monte Carlo or cluster-variation method (CVM) calculations could be performed with the $\epsilon^{(n)}$ of Eq. (4.1) to predict these temperatures, (see Secs. IV B and V). However, we found that a simple approximation, accurate to within 6% (see Appendix II) suffices for our purpose in this section, where this precision is adequate. For the simple fcc sys-

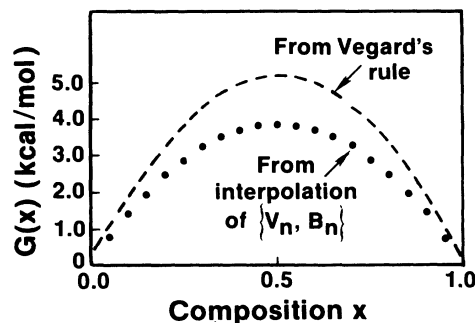


FIG. 1. The elastic energy $G(x) = \Omega x(1-x)$ for the Cu-Au system obtained by interpolating $\{V_n, B_n\}$ of the ordered compounds (Table II) with (a) a third-order polynomial (dots), and (b) linearly (i.e., using Vegard's rule, dashed line). Note that the use of Vegard's rule gives a much larger elastic energy.

tem $A_{1-x}B_x$ with ground states of the type AB (space group $L1_0$) and A_3B and B_3A (space group $L1_2$), CVM calculations can be performed for a large range of $\epsilon^{(n)}$ values; the resulting transition temperatures T_n for order-disorder transformations can then be fitted to $\epsilon^{(n)}$, providing the matrix A_{nm} in

$$\mathbf{T}_m = A_{mn} \epsilon^{(n)}, \quad (4.4)$$

where \mathbf{T}_m is a vector of transition temperatures and $\epsilon^{(n)}$ is the vector of the substitution energies. Appendix II gives this useful matrix [and discusses the precision of Eq. (4.4)] as well as corresponding fits for the critical compositions X_n and latent heats of transformation L_n . The matrix A_{mn} hence provides a quick way to estimate transition temperatures from a set of chemical energies. Since, for this system, accurate Monte Carlo calculations predict a T_2 which is lower by a factor $\eta = 0.967/1.026 = 0.9425$ than CVM results, if one wishes to compare the calculated T_2 with experiment, this factor has to be included in Eq. (4.4). Using our $\epsilon^{(n)}$ values [Eq. (4.1)] deduced from structural and thermodynamic data (Table II), Eq. (4.4) and the factor η , we predict for the CuAu system

$$\begin{aligned}\eta T_1 &= 747 \text{ K}, \\ \eta T_2 &= 683 \text{ K},\end{aligned}$$

TABLE II. Experimental molar volumes V_n , bulk moduli B_n , and formation enthalpies $\Delta H^{(n)}$ of the Ordered Structures for the $\text{Cu}_{1-x}\text{-Au}_x$ System.

n	Formula for definition of the mole	X_n concent.	V_n^a (cm^3/mol)	B_n^a (GPa)	$\Delta H^{(n)}$ (kcal/mol) ^b
0	Cu	0	7.112	138	0
1	$\text{Cu}_{0.75}\text{Au}_{0.25}$	0.25	8.294	148	-1.71
2	$\text{Cu}_{0.50}\text{Au}_{0.50}$	0.50	8.767	163	-2.10
3	$\text{Cu}_{0.25}\text{Au}_{0.75}$	0.75	9.506		-1.37 ^c
4	Au	1	10.218	171	0

^aSee Ref. 34.

^bSee Ref. 16.

^cObtained by interpolating enthalpies at $T = 800$ K and adding the ordering enthalpy—see Ref. 16.

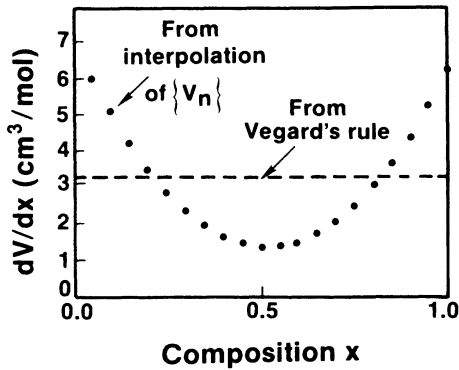


FIG. 2. dV/dx for the Cu-Au system obtained by taking the derivative of $V(x)$ (a) when $V(x)$ is a third-order polynomial interpolating $\{V_n\}$ (dots) and (b) when $V(x)$ follows Vegard's rule (dashed line).

in good agreement with the experimental data¹⁶ of $T_1=663$ K and $T_2=683$ K. This demonstrates that our theory can obtain $\{\varepsilon^{(n)}\}$, and through CVM calculations predict order-disorder transition temperatures using as input elastic and thermodynamic data of ordered phases alone.

One can further compare the ordering energies deduced from the thermodynamic data [Eq. (4.1)], with those obtained by Kikuchi *et al.*¹⁸ who fitted the observed CuAu phase diagram by adjusting $\varepsilon^{(n)}$ [with $G(x)\equiv 0$]. Their $\varepsilon^{(1)}, \varepsilon^{(2)}, \varepsilon^{(3)}$ values (after dividing by the factor η to account for the error in a CVM calculation relative to Monte Carlo) are

$$\begin{aligned}\varepsilon^{(1)} &= -4.236 \text{ kcal/mol}, \\ \varepsilon^{(2)} &= -5.592 \text{ kcal/mol}, \\ \varepsilon^{(3)} &= -3.858 \text{ kcal/mol},\end{aligned}\quad (4.5)$$

in excellent agreement with our results of Eq. (4.1) in which no fit to phase diagrams is involved. Note, however, that in the model of Kikuchi *et al.*¹⁸ the $\varepsilon^{(n)}$ values take up the role of enthalpies of formation $\Delta H^{(n)}$ (since all elastic interactions are neglected). Comparing, however, their $\varepsilon^{(n)}$ of Eq. (4.5) to $\Delta H^{(n)}$ of Eq. (4.3) shows clearly that this premise of their model is invalid: Their model cannot fit transition temperatures and enthalpies with any given set of $\varepsilon^{(1)}, \varepsilon^{(2)}$, and $\varepsilon^{(3)}$. We return to this point in the next section.

B. Phase diagrams of Cu-Au in the ε - G and ε -only approaches

To demonstrate the consequences of the interplay between chemical and elastic energies, we compare the calculated phase diagram and thermodynamic functions of the Cu-Au system in two ways: (i) retaining in Eq. (3.9) both chemical and elastic terms (the " ε - G approach"), or (ii) retaining just the chemical term (the " ε -only" or "pure-Ising" approach).

We use again the thermodynamic and structural data of Table II, but this time we also fit the observed¹⁶ transi-

tion temperature $T_1=663$ K, $T_2=683$ K, and $T_3\approx 500$ K for order-disorder transformations of Cu_3Au , CuAu , and CuAu_3 , respectively, to obtain a more accurate fit to the observed phase diagram. This is done as follows: for the bulk modulus we use the fit

$$B(x) = 43.251[V(x)]^{0.5914625}$$

(where B is given in GPa and V is in cm^3/mol). This form gives the correct values at the extremes $n=0$ (Cu) and $n=4$ (Au), and produces errors less than 5% for $n=1,2$. It is hence used to obtain the unmeasured B_3 . We obtain $V(x)$ by a polynomial interpolation of $\{V_n\}$ of Table II, as before. However, this time we also adjust the three derivatives dV/dx [see Eq. (3.10)] at the stoichiometric compositions $X_n = \frac{1}{4}, \frac{1}{2}$, and $\frac{3}{4}$. These derivatives are adjusted such that upon integration of $G(x)$ of Eq. (3.10), one obtains certain desired values of $G(X_n)$ at the stoichiometric compositions X_n . These values are fixed by the condition that $\varepsilon^{(n)} = \Delta H^{(n)} - G(X_n)$ [using $\Delta H^{(n)}$ values of Table II, and the correction factor η] produces the correct transition temperatures T_n . This yields³³

$$\begin{aligned}\varepsilon^{(1)} &= -4.024/\eta = -4.269 \text{ kcal/mol}, \\ \varepsilon^{(2)} &= -5.264/\eta = -5.585 \text{ kcal/mol}, \\ \varepsilon^{(3)} &= -3.628/\eta = -3.849 \text{ kcal/mol},\end{aligned}\quad (4.6)$$

where $\eta=0.9425$ is again the Monte Carlo-to-CVM ratio. These values are similar to those given in Eq. (4.1) in which no adjustments to fit critical data is involved. From Eq. (3.15) and using the $\Delta H^{(n)}$ values of Table II, this gives

$$\begin{aligned}G(X_1) &= 2.412/\eta = 2.559 \text{ kcal/mol}, \\ G(X_2) &= 3.285/\eta = 3.485 \text{ kcal/mol}, \\ G(X_3) &= 2.336/\eta = 2.479 \text{ kcal/mol}.\end{aligned}\quad (4.7)$$

The full $G(x)$ curve (solid line in Fig. 3) is obtained again by integrating Eq. (3.10) with our $V(x)$, $B(x)$, and dV/dx described above. For purposes of illustration [see Eqs. (3.12)–(3.14)] it suffices to represent this $G(x)$ curve by the simpler form $\Omega x(1-x)$ [solid dots in Fig. 3 and Eqs. (3.12)–(3.14)] with $\Omega=13.408/\eta=14.226$ kcal/mol, with virtually no loss in precision. The four values (ε and Ω) completely specify the Hamiltonian we use. (Note that in Ref. 33 the values of ε , G , and Ω were quoted before the division by η .) Note further that the common assumption of Vegard's rule ($dV/dx=\text{const}$) substantially overestimates G (dashed line in Fig. 3). We have calculated the phase diagrams⁴⁵ [Figs. 4(a) and 4(b)], and the enthalpy [Eq. (2.13)], at $T=800$ K [Fig. 5(a)] using the cluster variation method, retaining up to four-body (tetrahedron) interactions within the first nearest neighbors.⁴⁵ We show the results for the ε -only and the ε - G approaches in Figs. 4 and 5.

Since isostructural order-disorder transformations occurring at a fixed composition (hence volume) involve solely spin-flip chemical energies, both the ε - G and the ε -only approaches yield the same transition temperatures

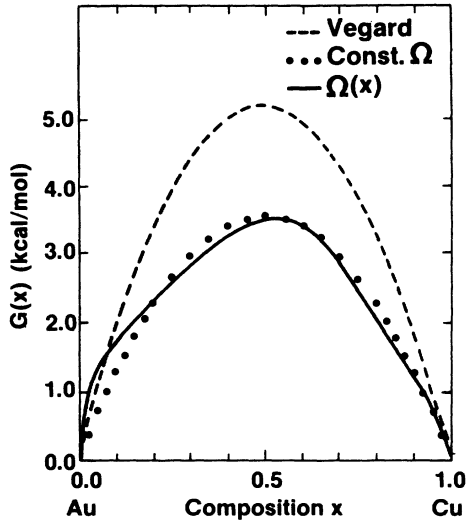


FIG. 3. The elastic energy $G(x)$ for the Cu-Au system obtained by fitting critical temperatures. (a) The best fit (full curve); (b) the $\Omega x(1-x)$ approximation with constant Ω (dots); (c) assuming Vegard's rule (dashed line).

[compare Figs. 4(a) and 4(b), where we obtain the transition temperatures 681.6, 676.1, and 497.4 K at the critical compositions 0.265, 0.497, and 0.727, for $n=1, 2$, and 3, respectively]. Thus, the higher-temperature parts of the phase diagrams of Figs. 4(a) and 4(b) are identical.

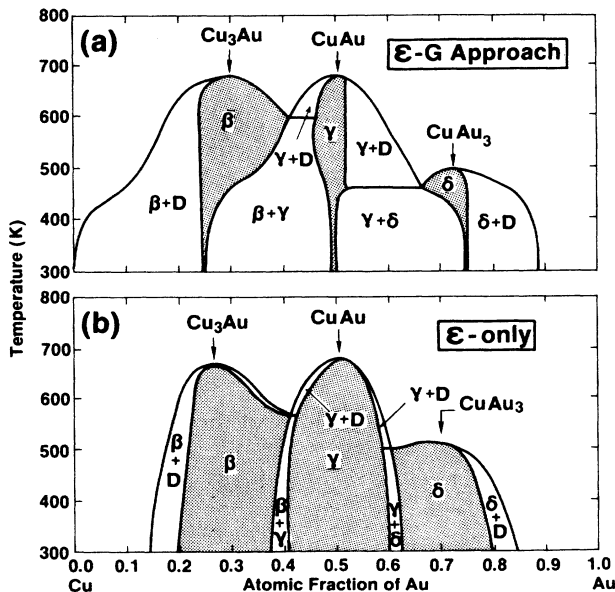


FIG. 4. CVM phase diagram for Cu-Au in the nearest-neighbor tetrahedron approximation: (a) in the ϵ - G approach, i.e., including both elastic and chemical interactions, using $\epsilon^{(n)}$ of Eq. (4.6) and $G(x)$ of Fig. 3 (constant Ω); (b) in the ϵ -only approach, i.e., neglecting the elastic interaction. Note that the single phase (two-phase) regions are much narrower (broader) in (a) relative to (b).

Comparison with the experimental results¹⁶ (available for Cu_3Au and CuAu only down to ~ 550 K and for CuAu_3 only down to ~ 470 K) reveals an overall good agreement (through our fit) for the top part of the phase diagrams in both approaches. A closer look at the slopes of the phase diagram lines away from the order-disorder transformation points reveals some subtle differences: whereas in the ϵ - G approach the triple point (where CuAu-I , CuAu_3 , and the disordered phase coexist) occurs at a composition of $\sim 67\%$ Au, close to the experimental value^{16(c)} of 66–67%, in the ϵ -only approach this point is too low (just below 60% Au). Another difference occurs in the CuAu_3 phase boundary line extending from 68% Au to the CuAu_3 order-disorder transition point at 72.7% Au: Whereas this line occurs in the ϵ -only approach at a nearly constant temperature, while in the ϵ - G approach this line shows a slight temperature increase in this composition range (by ~ 10 K), experimentally,^{16(c)} a decrease of ~ 22 K is observed. These differences are indeed subtle,

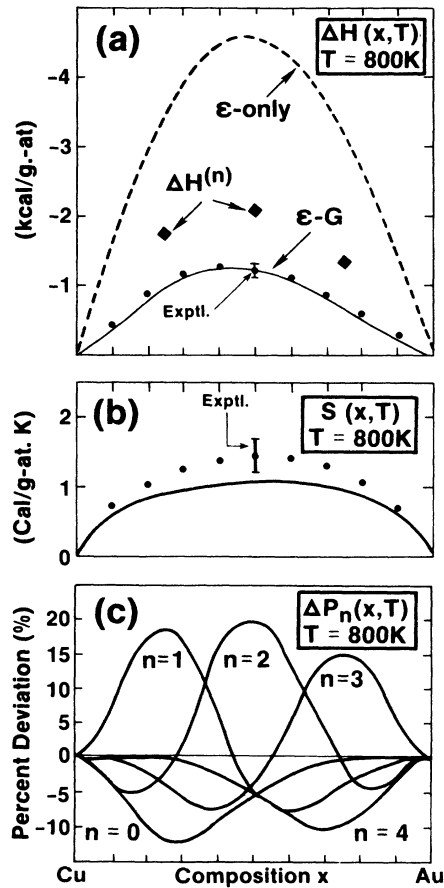


FIG. 5. (a) Enthalpy, (b) entropy, and (c) deviations from the random probabilities of the Cu-Au system at 800 K. Experimental data (Ref. 16) are shown as solid circles. The diamond-shaped symbols in (a) depict the observed formation enthalpies of the ordered phases (Table II). Note that the ϵ -only approach cannot account for the enthalpy. Note also that the entropy has a non-negligible contribution due to phonons, unaccounted for in our CVM calculation.

so we did not attempt to fit them any better (a fit is clearly easier in the ε - G approach having more parameters). On the other hand, the phase diagrams of ε - G and ε -only approaches are *radically* different in their lower temperature parts: In Fig. 5(a), the two-phase regions are very extended and the single-phase regions are very narrow, while in Fig. 5(b) the opposite is true.

Unfortunately, the phase diagram of Cu-Au was not measured at the temperatures where the difference is so striking (below 400 K). However, inspection of measured phase diagrams for other compound-forming metal alloys^{16(a)} leaves little doubt that, in general, the single-phase (ordered compound) regions (shaded areas in Fig. 4) tend to become *narrower* as the temperature is decreased [as in the ε - G case of Fig. 4(a)], rather than *broader* [as in the ε -only approach of Fig. 4(b)]. This seems to suggest a *qualitative* breakdown of the ε -only, pure-Ising approach. Further low-temperature experiments would be required to examine this point in detail.

In Fig. 5(a) we compare the calculated and measured mixing enthalpy of the disordered CuAu alloy at 800 K. Again we observe that the ε -only approach [dashed line in Fig. 5(a)] can in no way account for the observed mixing enthalpy when the chemical energies $\varepsilon^{(n)}$ are adjusted^{13,18} to give the correct transition temperatures. On the other hand, with the ε - G approach we can fit both transition temperatures and enthalpy. Note also in Fig. 5(a) that due to strain energy the formation enthalpies of the *ordered* phases [diamond-shape symbols in Fig. 5(a) giving $\Delta H^{(n)}$ of Table II] are far smaller than the mixing enthalpy of the *disordered* phase, as argued previously by Srivastava *et al.*²²

It is important to realize that our decomposition of the formation enthalpy $\Delta H^{(n)}$ of ordered phases into a chemical ($\varepsilon^{(n)}$) and elastic [$G(X_n)$] terms holds the key to distinguishing phenomena that depend on $\{\varepsilon^{(n)}\}$ alone from those that depend also on $G(x)$. As indicated above, phenomena that connect phases at the same composition are affected by $\varepsilon^{(n)}$ alone. These include not only the order-disorder transitions at fixed-compositions, but also all measurables that reflect the relative probabilities $P_n(x, T)$ of Eq. (2.12). Since the *relative* energies $\Delta E(n, V)$ of different clusters n at a given $V = V(x)$ do not depend on $V(x)$, the cluster probabilities $P_n(x, T)$ depend on $\{\varepsilon^{(n)}\}$ alone. Hence, the knowledge of the stability $\Delta H^{(n)}$ of an ordered compound does not suffice to determine whether an alloy would show "clustering" of its constituents [$\varepsilon^{(n)} < 0$, making $P_n(x, T)$ for $n = 1, 2$, and 3 *larger* than the random (R) probability $P_n^{(R)}(x)$ at $x = X_n$] or "anticlustering" [$\varepsilon^{(n)} > 0$, making $P_n(x, T) < P_n^{(R)}(X_n)$]. This explains why in previous calculations $\text{In}_x\text{Ga}_{1-x}\text{As}$ alloys^{25(a)} were predicted to exhibit anticlustering but calculations^{25(b)} on $\text{Cd}_{1-x}\text{Zn}_x\text{Te}$ predicted "clustering," despite the fact that $\Delta H^{(n)} > 0$ for *both* systems and all values of n : the former system has^{25(a)} $\varepsilon^{(n)} > 0$, whereas the latter has $\varepsilon^{(n)} < 0$.

Figure 5(c) shows our calculated deviation from randomness $\Delta P_n(x, T) = P_n(x, T) - P_n^{(R)}(x)$ for Cu-Au at $T = 800$ K and exhibits clustering (excess of Cu_3Au , CuAu , and CuAu_3 at $x = \frac{1}{4}$, $\frac{1}{2}$, and $\frac{3}{4}$, respectively) since the $\varepsilon^{(n)}$'s are negative. The configurational entropy ob-

tained from our $P_n(x, T)$ is compared in Fig. 5(b) with experiment.¹⁶ The good agreement with experiment (which, however, contains also small electronic and vibrational entropies) demonstrates again the utility of our approach in predicting *thermodynamic* data (ΔH , ΔS) from *critical data* (fitting transition temperatures).

C. Mixing enthalpies of semiconductor alloys

Another system where we can compare our theoretical formulation with experiment is the case of compound semiconductors. Contrary to the situation in many metallurgical systems, detailed thermodynamic data are not available for semiconductor alloys, except at high temperatures. For instance, we do not know the enthalpies of formation of the ordered intermediate compounds, even if they are stable. The observed high-temperature mixing enthalpy of disordered semiconductor alloys has been successfully approximated by Stringfellow³⁷ with a universal equation

$$\Delta H^{(D)}(x) \equiv \hat{\Omega}x(1-x),$$

where the effective interaction parameter $\hat{\Omega}$ [not to be confused with the elastic interaction parameter Ω of Eqs. (3.13) and (3.14)] is

$$\hat{\Omega} \cong 5.03 \times 10^4 (\Delta a)^2 / a^{4.5}. \quad (4.8)$$

Here, the mixing enthalpy $\Delta H^{(D)}$ is given in kcal/mol, a is the average lattice parameter of the constituents (in Å), and Δa is the absolute value of the lattice parameter difference between the pure constituent semiconductors. Equation (4.8) was shown³⁷ to hold well for a whole series of IV-IV and III-V ("isovalent") semiconductors. We will show that this phenomenological equation, derived for the high-temperature limit by assuming³⁷ Vegard's rule,³² can be simply obtained as a particular case of our general expression in Eqs. (3.9) and (3.10) under similar conditions, i.e., by assuming (i) random probabilities at high temperatures and (ii) Vegard's rule.

With the approximation (3.12), Eq. (3.9) becomes

$$\Delta E(\sigma) = \Omega x(1-x) + \sum_n \xi_n(\sigma) \varepsilon^{(n)}, \quad (4.9)$$

where by Eq. (3.15)

$$\varepsilon^{(n)} = \Delta H^{(n)} - \Omega X_n(1-X_n) \quad (4.10)$$

and $X_n = n/4$ is the composition of the ordered structure $A_n B_{4-n} C_4$ (e.g., $\text{In}_x\text{Ga}_{1-x}\text{As}$ alloys can order in $\text{In}_n\text{Ga}_{4-n}\text{As}_4$ phase²⁴). Combining Eq. (4.9) and (4.10) gives

$$\Delta E(\sigma) = \Omega \left[x(1-x) - \sum_n X_n(1-X_n) \xi_n(\sigma) \right] + \sum_n \Delta H^{(n)} \xi_n(\sigma). \quad (4.11)$$

In Eq. (4.11), the first term represents the "average medium" with concentration x , the last term represents the contribution of clusters n , whereas the second term can be thought of as a "medium-cluster" interaction term. When the cluster has an infinite size (making up the en-

ture system), only the last term exists. The practical question is how to select clusters of manageable sizes which represent well the physics at hand. We find that $M=4$ (tetrahedron) is the smallest cluster size for which the superposition model of Eq. (2.6), interpreted as a statistical mixture of periodic structures, is valid (i.e., there are states of order σ which can be described by rotations of the point groups of the ordered structures n). The choice of $M=4$ is also particularly suited for semiconductors, as the strongest (covalent) interactions are included within a C-atom-centered nearest-neighbor tetrahedra.

Equations (4.9) and (4.11) have a formal resemblance to those used by Bublik *et al.*,³⁰ in that the chemical and elastic effects are separated. Note that the first two terms in the large parentheses of Eq. (4.11) exhibit a partial cancellation, which would result (see below) in a substantial reduction in the elastic energy of the alloy. [This reduction is, however, unrelated to the reduction by the Poisson ratio involved by Krivoglaz²⁶ or to the use of unphysically soft energies $\Delta E(n, V)$ by Chen and Sher²⁵ (their Fig. 2)]. Using our $\Delta E(\sigma)$ of Eq. (4.11) with the definition of the mixing enthalpy $\Delta H^{(D)}$ of the disordered alloy [Eq. (3.5)] we obtain

$$\begin{aligned} \Delta H^{(D)}(x, T) &= \langle \Delta E(\sigma) \rangle \\ &= \Omega \left[x(1-x) - \sum_n P_n(x, T) X_n (1-X_n) \right] \\ &\quad + \sum_n P_n(x, T) \Delta H^{(n)}. \end{aligned} \quad (4.12)$$

At the high-temperature limit, [where $\Delta H^{(D)}(x, T)$ for semiconductors are normally obtained experimentally^{36,37}] one can replace $P_n(x, T)$ by the random (Bernoulli) probability for four-atom clusters

$$P_n(x, \infty) = \langle \xi_n(\sigma) \rangle = \binom{4}{n} x^n (1-x)^{4-n}. \quad (4.13)$$

Note that $\langle \xi_n(\sigma) \rangle$ can be replaced here, by only the four-atom probabilities $P_n(x, T)$ ($0 \leq n \leq 4$) since we have retained the energies $\varepsilon^{(n)}$ up to four-body terms. Higher multiatom interactions (e.g., tetrahedron-tetrahedron) have smaller n -atom interaction energies J_n , hence, their contribution to Eqs. (4.9) and (4.10) is expected to renormalize the values of the tetrahedron $\varepsilon^{(n)}$ s. The property of Eq. (4.13) is that for $X_n = n/4$ one has⁴⁶

$$\sum_n P_n(x, \infty) X_n (1-X_n) = \frac{3}{4} x(1-x), \quad (4.14)$$

hence Eq. (4.12) gives

$$\Delta H^{(D)}(x, \infty) = \frac{\Omega}{4} x(1-x) + \sum_n P_n(x, \infty) \Delta H^{(n)}. \quad (4.15)$$

The important feature of Eq. (4.15) is that *the elastic energy is reduced by a factor of four due to the statistical cancellation between the alloy elastic energy $G(x)$ [first term in large parentheses in the right-hand side of Eq. (4.12)] and the elastic energy at stoichiometric compositions [second term in large parentheses in Eq. (4.12)].*

The elastic interaction parameter Ω can be simply estimated from Eq. (3.14) by using Vegard's rule,³² which is followed rather closely by most semiconductor alloys. Denoting by $V = N_0 a^3/4$ the molar volume, where a is the cubic lattice parameter and N_0 is Avogadro's number, Vegard's rule implies

$$\frac{dV}{dx} = \frac{3}{4} N_0 a^2 \Delta a, \quad (4.16)$$

where Δa is the lattice mismatch. Using a constant ratio B/V , Eq. (3.14) can be integrated to give

$$\Omega = \frac{9}{2} B V \left[\frac{\Delta a}{a} \right]^2. \quad (4.17)$$

Eq. (4.17) is exactly the "unrelaxed" interaction parameter of Fedders and Muller.³¹ Those authors found that they had to divide their Ω by a factor of about four to account for the observed mixing enthalpy. No such *ad hoc* factor is needed here. Using Eq. (4.15) and (4.17), we find that when Vegard's rule is satisfied, the high-temperature mixing enthalpy is

$$\begin{aligned} \Delta H^{(D)}(x, \infty) &= \frac{9}{8} \left[B V \frac{(\Delta a)^2}{a^2} \right] x(1-x) \\ &\quad + \sum_n P_n(x, \infty) \Delta H^{(n)}. \end{aligned} \quad (4.18)$$

This is our general expression for the high-temperature mixing enthalpy of semiconductor alloys; it demonstrates, as shown earlier,²² that (since the first term on the right-hand side is non-negative) $\Delta H^{(X_n)} > \Delta H^{(n)}$.

This equation can be further simplified for *isovalent semiconductor alloys* by noting that they have very small^{22,23,47,48} (positive or negative) formation enthalpies $\Delta H^{(n)}$, of the order of ± 0.2 kcal/mol whereas $\Delta H^{(D)}(0.5)$ is about 10 times larger.³⁷ This results primarily from the fact that both constituents are *closed-shell octet compounds* (hence, nearly inert). Indeed, calculations on AlAs-GaAs,⁴⁷ GaP-InP,²² CdTe-MnTe,⁴⁸ and HgTe-CdTe,⁴⁷ show $|\Delta H^{(n)}| \approx 10-20$ meV/atom-pair. We will hence neglect this term in Eq. (4.18). It is important to note, however, that $\Delta H^{(n)} \approx 0$ holds only if one properly relaxes the cell-internal degrees of freedom^{22,47,48} (in the present case, the position of the common atom C inside its $A_n B_{4-n} C_4$ tetrahedron). Neglecting $\Delta H^{(n)}$ gives for Eq. (4.18) the high-temperature mixing enthalpy

$$\Delta H^{(D)}(x, \infty) = \frac{\Omega}{4} x(1-x) \cong \left[\frac{9}{8} B V \left[\frac{\Delta a}{a} \right]^2 \right] x(1-x), \quad (4.19)$$

$$\hat{\Omega} \equiv \Delta H^{(D)}(x, \infty) / x(1-x) = \frac{9}{8} B V (\Delta a / a)^2. \quad (4.20)$$

One sees that the empirical factor of about four used by Fedders and Muller is wholly statistical in nature. As we will see below, Eq. (4.20) forms an excellent estimate of the high-temperature mixing enthalpy of many semiconductor alloys.

It is worth noting at this point that whereas $\Delta H^{(n)} \cong 0$ is appropriate for isovalent semiconductor alloys, $\varepsilon^{(n)} \cong 0$ is not. As described in Sec. III A [text surrounding Eq. (3.2)], the chemical energy $\varepsilon^{(n)}$ includes, in the case where a common sublattice C exists, also the energy lowering due to the relaxation of this common sublattice [in the terminology of Ref. 22, our $\varepsilon^{(n)}$ equals their $\Delta E_{CE} + \Delta E_S$]. Hence, when a large lattice mismatch exists between the constituents AC and BC , the C sublattice relaxes substantially,²⁹ leading generally to a large reduction in $\varepsilon^{(n)}$, hence $\varepsilon^{(n)} \cong 0$ is inappropriate. In fact, using in Eq. (4.18) the condition $\varepsilon^{(n)} = 0$ gives by Eq. (4.10)

$$\Delta H^{(n)} = \Omega X_n (1 - X_n) \text{ for } \varepsilon^{(n)} = 0. \quad (4.21)$$

Using Eq. (4.18) and (4.14) then yields

$$\Delta H^{(D)}(x, \infty) = \frac{9}{2} B V \left[\frac{\Delta a}{a} \right]^2, \text{ for } \varepsilon^{(n)} = 0. \quad (4.22)$$

an unphysical result, 4 times larger than the correct result [Eq. (4.19)]. The reason that $\Delta H^{(n)} \cong 0$ is a reasonable approximation is precisely that a large negative $\varepsilon^{(n)}$ which exists when substantial common-sublattice relaxation occurs is offset by the elastic term $G(x)$. The reason that $\varepsilon^{(n)} \cong 0$ is not satisfied in general (except for $\Delta a = 0$) is that ε includes the non-negligible energy lowering due to relaxation of the C sublattice for a fixed A, B lattice.

Equation (4.19) could be used to calculate the enthalpy of mixing from the knowledge of B , V , and Δa of the alloy. One could, however, further simplify it to eliminate B and V by using the scaling relation between the bulk modulus and the lattice parameter⁴⁹

$$B = \frac{3.30 \times 10^4}{a^{3.5}} \quad (4.23)$$

(where B is in GPa, and a in Å). Inserting this in Eq. (4.20) gives

$$\hat{\Omega} = 1.34 \times 10^3 a^{-2.5} (\Delta a)^2 \quad (4.24)$$

($\hat{\Omega}$ in kcal/mol, a in Å). Comparing this result with that of Stringfellow, [termed the ‘‘Delta lattice parameter’’ or DLP model and given by Eq. (4.8)] we find the ratio

$$\frac{\hat{\Omega}(\text{present})}{\hat{\Omega}^{(D)}(\text{DLP})} = 0.0266 a^2. \quad (4.25)$$

The ratio given by Eq. (4.25) varies between 0.79 (Si) to 1.13 (InSb). Thus, within the experimental uncertainty in $\Delta H^{(D)}$ (unfortunately, for semiconductor alloys this uncertainty is as large as $\pm 50\%$), Eqs. (4.25) and (4.8) are indistinguishable. However, unlike Stringfellow’s DLP model, no empirical scaling of the enthalpy is needed.

V. REMOVAL OF $T=0$ DEGENERACY BY ELASTIC EFFECTS: MODEL HAMILTONIAN CALCULATIONS

To understand how the elastic energy influences the phase diagram, we now study the free energy defined at $T=0$ by Eq. (4.9), considering $\Delta E(\sigma)$ as the Hamiltonian for the state of order variables σ . To simplify matters,

we consider a fcc binary alloy in the simple cubic superlattice retaining just the ‘‘pair interaction.’’ This means that, for the ordered fcc structures $A_n B_{4-n}$ (see Table II), we set

$$\Delta H^{(1)} = \Delta H^{(3)} = 0.75 \Delta H^{(2)}. \quad (5.1)$$

According to Eq. (3.15), one also has

$$\varepsilon^{(1)} = \varepsilon^{(3)} = 0.75 \varepsilon^{(2)}. \quad (5.2)$$

The minimum energy of Eq. (4.9) occurs when all probabilities $\xi_n(\sigma)$ are zero, except for two, say ξ_N and ξ_M , for which

$$\xi_N + \xi_M = 1, \quad (5.3)$$

and

$$X_N \xi_N + X_M \xi_M = x. \quad (5.4)$$

Thus

$$\xi_M = \frac{x - X_N}{X_M - X_N}, \quad \xi_N = \frac{x - X_M}{X_N - X_M}. \quad (5.5)$$

The ground state energy $\Delta E(x)$ of the alloy then becomes by Eq. (4.9)

$$\Delta E(x) = \Omega x(1-x) + \varepsilon^{(N)} \frac{x - X_M}{X_N - X_M} + \varepsilon^{(M)} \frac{x - X_N}{X_M - X_N}. \quad (5.6)$$

At the compositions $x = X_N$ of the ordered structure, the equilibrium energy is the enthalpy of formation of this phase, i.e.,

$$\Delta E(X_N) = \Omega X_N (1 - X_N) + \varepsilon^{(N)} \equiv \Delta H^{(N)}. \quad (5.7)$$

Between these compositions, the second derivative is a negative constant:

$$\frac{d^2 \Delta E}{dx^2} = -2\Omega. \quad (5.8)$$

In Figs. 6(a) and 6(b) we plot $\Delta E(x)$ of Eq. (5.6). Figure 6(a) refers to the case when the enthalpies of formation of Eq. (5.7) are negative (stable compounds), while in Fig. 6(b) the formation enthalpies are positive. In both figures, the dashed lines denote the energy $\Delta E(x)$ for the pure Ising model, i.e., when we set $\Omega = 0$ in Eq. (4.9). The pure (‘‘ ε -only’’) Ising Hamiltonian produces an infinite degeneracy in the ground state. This is observed as follows. Consider the point denoted as x in Fig. 6(a). This state has the same energy as a mixture of states y with z , if these are mixed in the proportions

$$\frac{z-x}{z-y} \text{ for } y \text{ and } \frac{x-y}{z-y} \text{ for } z.$$

No such degeneracy exists when we include the elastic energy Ω (solid curves in Fig. 6).

Returning to the phase diagrams of Fig. 4, one sees that the narrowness of the single-phase regions in the ε - G approach [Fig. 4(a)] reflects the ground state of Fig. 6(a) with its very sharp minima. In contrast, the broadness of

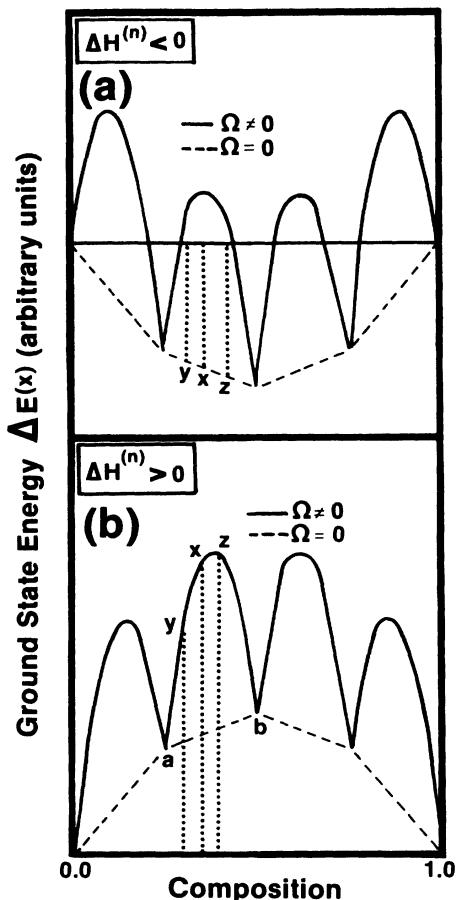


FIG. 6. Ground-state energy as function of composition for the simple model of Eq. (5.6). (a) Negative formation enthalpies $\Delta H^{(n)}$ for the intermediate ordered compounds. (b) Positive $\Delta H^{(n)}$'s. Observe that the elastic energy stabilizes the compounds by making the nonstoichiometric compositions energetically unfavorable.

the single-phase regions in the ϵ -only approach [Fig. 4(b)] reflects the infinite degenerate ground state represented by the dashed lines in Fig. 6(a). Real phase diagrams^{16(a)} of compound forming systems show ordered compounds at narrowly defined near-stoichiometric compositions, in sharp contrast with the predictions of the ϵ -only model, which yields at low temperatures broad composition ranges for ordered phases (using *any* combination of $\epsilon^{(1)}$, $\epsilon^{(2)}$, and $\epsilon^{(3)}$). For this reason we find the approach which includes elastic energies [Fig. 4(a)] to be a better description of actual phase diagrams than the pure Ising ϵ -only approach [Fig. 4(b)].

VI. ELASTIC EFFECTS ON THE TRIPLE POINT: MODEL HAMILTONIAN AND ITS SOLUTIONS

There has been considerable controversy regarding the location of the triple point in CVM and Monte-Carlo solutions to the pure, ϵ -only Ising model.^{19,20,50} We show here that the CVM and Monte Carlo solutions to the

more realistic ϵ - G Hamiltonian yield essentially the same results, and that the triple point is *raised* by introducing in the Hamiltonian an elastic, $G(x)$ term. A mechanism for such an increase in the triple-point temperature has been sought in the past,⁵⁰ since nearly exact solutions to the ϵ -only Ising Hamiltonian produced a triple point which is decisively *lower* than what was observed^{16(b),16(c)} for the Cu-Au (and other) systems. The position of the triple point (when equilibrium exists between the disordered, the AB and the AB_3 phases) is related to the infinitely degenerate ground state of the pure Ising model (dashed curves in Fig. 6). Since $G(x)$ removes much of this degeneracy (solid curves in Fig. 6), it seems worthwhile to investigate if elastic effects might also raise the triple point significantly above $T=0$.

We demonstrate this point by applying the Monte Carlo (MC) method to a simple model Hamiltonian.⁵¹ In Figs. 7(a), for $G(x)=0$ (or $\Omega=0$), and 7(b) for $G(x)\neq 0$ or ($\Omega\neq 0$), we show the results of MC calculations at fixed temperature. We chose a model Hamiltonian with pair interaction $\epsilon^{(1)}=\epsilon^{(3)}=0.75\epsilon^{(2)}=-6.0$ kcal/mol, and the simplest form for $G(x)=\Omega x(1-x)$, with Ω chosen so that the enthalpies of formation $\Delta H^{(n)}=\Omega X_n(1-X_n)+\epsilon^{(n)}$ were very small negative numbers (Fig. 7). In the Monte Carlo calculations we use a periodic crystal with 8^3 conventional unit cells (thus with $4\times 8^3=2048$ atomic sites). Spin flips are made sequentially at the atomic sites along the lattice. The spin-flip energy is calculated by counting the tetrahedra. We verified that, in most cases, after starting from any state of order, the spin-flip process reached a stationary state in 200 flip attempts per site. In Figs. 7(a) and 7(b) the solid circles have sizes larger than the actual errors in the calculated averages of 100 flip attempts per site, after reaching the stationary condition. In no instance did we need to go beyond the total of 500 flip attempts/site.

In Fig. 7(a) [for $G(x)=0$] one finds *two* phase transitions obtained in the MC calculation at $T=700$ K: AB -to-disorder at $\mu\cong 5$ kcal/mol and disorder-to- AB_3 at $\mu=10$ kcal/mol. The values of the chemical potential μ at the phase transitions are in agreement with those calculated by Binder *et al.*⁵⁰ In order to compare their results with ours, we transform their variables [see their Eq. (2.8)]

$$\frac{k_B T}{|J_{nn}|} = \frac{8RT}{|\epsilon^{(2)}|} = 1.39$$

and

$$\frac{H}{|J_{nn}|} = \frac{4\mu}{|\epsilon^{(2)}|} = \frac{\mu}{2}.$$

The first phase transition, at $\mu\cong 5$ kcal/mol, is clearly first-order, while that at $\mu\cong 10$ kcal/mol seems to present a very negligible discontinuity (but very clear discontinuity in the slope). (Binder *et al.* claim that this second transition is also first-order, a feature that can be found only by increasing the number of spin flips, or by calculating at a more favorable temperature.) In Fig. 7(a) we also show the CVM result, which exhibits just a single phase transition. Except in the disordered phase region,

the CVM results follow the MC result very closely. Clearly, CVM and MC solutions to the same, pure-Ising Hamiltonian give qualitatively different answers.

In Fig. 7(b) we present the results for $G(x) \neq 0$. In this case, the MC and CVM results almost coincide, and there is just one phase transition (AB to AB_3), at $\mu = 0.8$ kcal/mol, clearly of first-order. Below and above the critical chemical potential μ , phases AB and AB_3 seem to be perfectly ordered ($P_2 = 1$ and $P_3 = 1$, respectively). The fact that the transition now occurs at a much smaller value of μ results from the important negative contribu-

tion dG/dx to the chemical potential.⁵¹ The Monte Carlo results in the case of $G(x) \neq 0$ [Fig. 7(b)] are actually more complicated than what is represented in the figure. Starting from different states of order, and with different spin-flip histories, we did get either a phase with $P_2 = 1$ and $P_3 = 0$, or a phase with $P_2 = 0$ and $P_3 = 1$, but never a disordered phase with intermediate probabilities. Once a given phase is reached, it will not move towards the other, even if it has larger free energy (metastability), because the acceptance ratio of spin flips per attempt becomes much too small ($\sim 1\%$). Thus, it was possible to

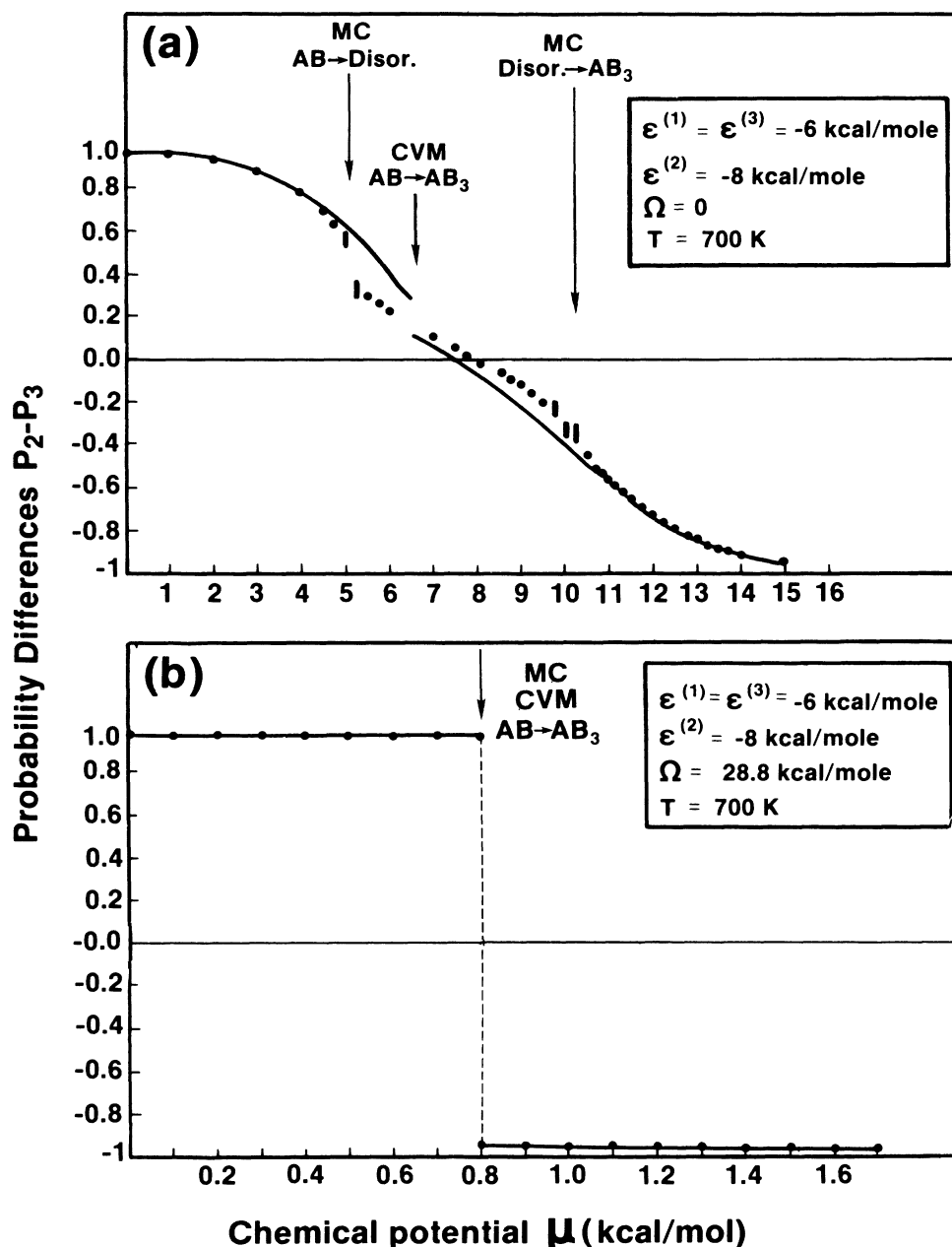


FIG. 7. (a) Difference of tetrahedron probabilities $P_2 - P_3$ as function of the chemical potential μ in a model Hamiltonian (parameters given in insert) for the ϵ -only approach. The solid curve is from the cluster variation method (CVM) calculation. The dots and bars are Monte Carlo (MC) results. Observe that there are two phase transitions in the MC calculation, but just one in the CVM approximation. (b) Results for the (ϵ, G) approach. Note that only a single phase transition is observed.

obtain the AB phase even for μ as high as $+1.1$ kcal/mol, and to obtain the AB_3 phase at μ lower than 0.8 . Thus, to decide which phase is more stable at a given μ , we compared the values of $U - \mu x$, where U is the internal energy. Since both phases have negligible entropy, this expression is approximately the value of the free energy, the lower value indicating the more stable phase. Our Monte Carlo calculations completely exclude the existence of an intermediate disordered phase at $T = 700$ K. Therefore, the triple point must be above this temperature if elastic energy is included.

During the MC work it was easy to verify that $G(x)$ does not remove completely the ground-state degeneracy of the Ising model. Although the phases had the tetrahedron probabilities $P_2 = 1$ and $P_3 = 0$ (or $P_2 = 0$ and $P_3 = 1$), the concentrations of atoms B in the four fcc sublattices did not assume the integer values, 0 or 1 , but could assume different noninteger values depending on the spin-flip history. The degeneracy not removed by $G(x)$ results from the possibility of arranging tetrahedra A_2B_2 (and AB_3) in different ways. In Fig. 8 we show the

possibilities. First consider Fig. 8(a), where we present the case of AB_3 . The circles are atoms in the plane of the figure and the triangles are in the neighboring plane. A solid figure (\bullet or \blacktriangle) is a B atom, while an empty figure (\circ or \triangle) is A . The tetrahedra, which are formed by four adjacent atoms, two in each plane, are all of the type AB_3 . One sees that there are planes of just B atoms, and planes where A and B alternate (planes α, β, γ). Lacking a next-nearest-neighbor interaction, the Hamiltonian is incapable of correlating the arrangement of atoms in consecutive AB planes. Thus one sees from Fig. 8 that there are two possible arrangements for each AB plane. Letting P be the number of such planes in the whole crystal, the degeneracy is then 3×2^P , where 3 is the number of crystallographic directions perpendicular to the ordered planes. The case of A_2B_2 [Fig. 8(b)] is similar, the only difference being that the number of ordered planes ($\alpha, \beta, \dots, \rho$) is twice as large.

VII. METASTABLE LONG-RANGE ORDERED COMPOUNDS FOR $\Delta H^{(n)} > 0$

A. The basic idea

The existence of a well-defined crystalline compound is traditionally taken to imply that its formation enthalpy is negative. In many cases, this necessary condition is not sufficient: One also requires that possible competing structures (not necessarily its constituent elements) are less favorable. We show here that *when elastic energies are significant* (e.g., when a large lattice mismatch exists between the constituent elemental solids) *one can obtain metastable ordered compounds even if the formation enthalpy is positive*.

Figure 6(b) presents an essential feature of the Hamiltonian with elastic energy. In this figure, the enthalpy of formation of the ordered structures $\Delta H^{(n)}$ is taken to be positive, so that a decomposition resulting in a mixture of the two pure end-point constituents might be expected at low temperatures. On the other hand, the *kinetics* of the decomposition may be such that the result could differ from *thermodynamic* expectation. Consider the point denoted x in Fig. 6(b). The decomposition progresses with the motion of the atoms in the lattice. Now, atoms do not make long jumps simultaneously, so that the composition of any small volume of material cannot suddenly change by large amounts. If we understand the decomposition as a continuous process of disproportionation, in the first stages, x would disproportionate into neighboring compositions y and z , and these would progress towards the points a and b . But at these points, there cannot be any further progress, because a motion towards the extremes $x = 0, 1$ would necessarily pass through compositions with higher energies. This means that a and b would appear to be "stable compounds," due to the impossibility of finding a path to a lower energy state. Thus, *the elastic energy opens the possibility of finding metastable long-range ordered compounds when $\epsilon^{(n)}$ is attractive (negative), even if the compound enthalpy of formation is positive*. Obviously, such solutions do not exist in the pure (ϵ -only) Ising model (dashed lines in Fig. 6).

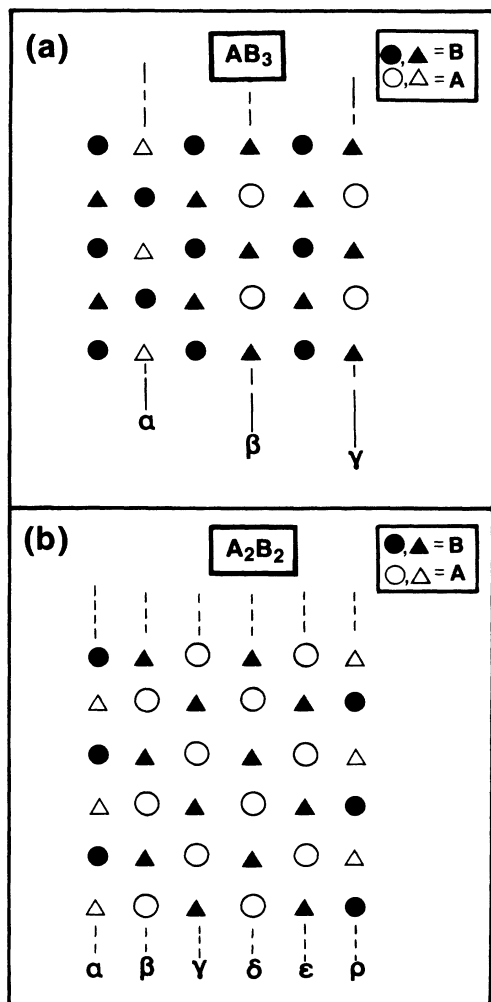


FIG. 8. Residual degeneracy of (a) AB_3 and (b) A_2B_2 for a model Hamiltonian with nearest-neighbor interaction. The AB planes $\alpha, \beta, \gamma, \dots, \rho$ are ordered, but their order is uncorrelated.

B. Phase diagram for strain-induced metastable compounds

To illustrate the metastability of ordered compounds brought by the elastic term $G(x)$, we calculated the CVM phase diagram of a model with *positive enthalpies* $\Delta H^{(n)}$ but *negative chemical energies* $\epsilon^{(n)}$ (Fig. 9). The phase diagram presents a very broad miscibility gap (solid line) starting at $T=1987$ K (obtained from the CVM), or 1920 K (obtained in the calculation MC). We have verified the limits of existence of the ordered phases γ and δ (dotted lines) inside this miscibility gap. These are defined by the condition

$$\frac{\partial^2 F}{\partial x^2} = 1 / \frac{\partial x}{\partial \mu} = 0, \quad (7.1)$$

where F is the Helmholtz free energy of the *ordered phase*, and the derivatives are taken at constant temperature T . When Eq. (7.1) is satisfied, not only does $\partial x / \partial \mu$ become infinite, but so does the heat capacity $T \partial S / \partial T$. (Here, the CVM natural iterations⁴¹ diverge from the ordered phase to converge to the A -rich, or B -rich disordered phase.) Despite the singularity in $\partial x / \partial \mu$, the dotted line in Fig. 9 could be determined with very good precision. One sees that *the ordered phases are metastable in a very narrow composition range even though thermodynamically they should not exist* (since $\Delta H^{(n)} > 0$). This is a consequence of the sharpness of the minima in Fig. 6(b).

In order to verify that Eq. (7.1) is truly the limit of metastability, we performed Monte Carlo calculations, in a periodic crystal with $4 \times 8^3 = 2048$ sites, starting from perfectly ordered γ and δ phases. After a total of 500 flip

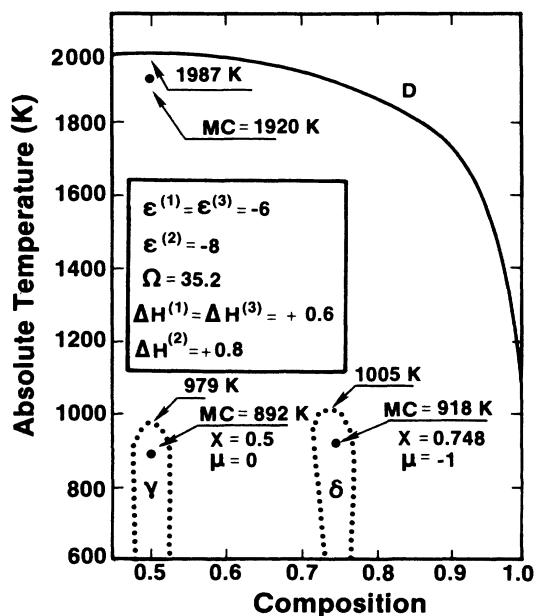


FIG. 9. CVM phase diagram for an alloy with positive enthalpy. Inside the dotted lines, the ordered phases are metastable (see text). Also shown are the Monte Carlo (MC) results as solid circles.

attempts/site we computed the average probability P_n of occurrence of a tetrahedron $A_{4-n}B_n$ to see how ordered the crystal remained. In Fig. 10 we show the results for the case of the phase γ . Very clearly there is a critical temperature (892 ± 1 K) above which the order disappears. The Monte Carlo critical temperatures (at selected values of the chemical potential), marked in the phase diagram of Fig. 9 as solid dots, do not differ by more than 9% from the CVM results calculated according to Eq. (7.1). This is a remarkable fact, showing that the CVM expression for the entropy is also reliable for calculating ordered phases.

C. Limits of stability and metastability

We now consider the necessary conditions for the existence of a stable or metastable phase with stoichiometric composition X_n [e.g., points a and b in Fig. 6(b)]. If one considers a disproportionation of X_n into neighboring compositions $X_n - \rho$ and $X_n + \omega$, the composition X_n will be stable (or metastable) if this process raises the energy of the alloy, or

$$\Delta E(X_n) < \frac{\rho}{\rho + \omega} \Delta E(X_n - \omega) + \frac{\omega}{\rho + \omega} \Delta E(X_n + \rho). \quad (7.2)$$

Since ρ and ω are small positive numbers, we can expand the right-hand side of this inequality to obtain the condition for stability or metastability in terms of the right and left derivatives at the stoichiometric compositions.

$$\left. \frac{d\Delta E}{dx} \right|_{x=X_n^+} - \left. \frac{d\Delta E}{dx} \right|_{x=X_n^-} > 0. \quad (7.3)$$

From Eq. (5.6) we obtain these derivatives

$$\left. \frac{d\Delta E}{dx} \right|_{x=X_n^+} = \Omega(1 - 2X_n) + \frac{\epsilon^{(n)} - \epsilon^{(n+1)}}{X_n - X_{n+1}} \quad (7.4a)$$

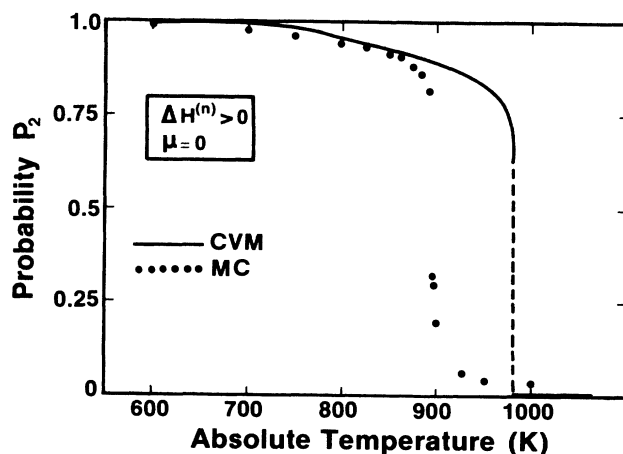


FIG. 10. Probability of the tetrahedron A_2B_2 in the metastable ordered phase AB as function of temperature. Each Monte Carlo calculation started from the perfectly ordered structure AB , and consisted of a run of 500 flip attempts/site. The dots are averages over the runs (their size has no significance). The solid line is the CVM result. The parameters used were $\epsilon^{(1)} = \epsilon^{(3)} = -6$; $\epsilon^{(2)} = -8$ and $\Omega = 35.2$ kcal/mol.

and

$$\left. \frac{d\Delta E}{dx} \right|_{x=x_n^-} = \Omega(1-2X_n) + \frac{\epsilon^{(n)} - \epsilon^{(n-1)}}{X_n - X_{n-1}}. \quad (7.4b)$$

Thus, Eq. (7.2) implies

$$2\epsilon^{(n)} - \epsilon^{(n+1)} - \epsilon^{(n-1)} < 0. \quad (7.5)$$

In the case of pair interactions $\epsilon^{(1)} = \epsilon^{(3)} = 0.75\epsilon^{(2)}$, Eq. (7.5), when applied to $n=1,2$, and 3 means that the necessary condition for both stability and metastability is

$$\epsilon^{(2)} < 0. \quad (7.6)$$

If, in addition, the ordered structures are stable relative to the constituents ($\Delta H^{(2)} < 0$), we have the conditions for relative stability of an ordered system with pair interactions

$$\epsilon^{(2)} < 0; \Delta H^{(2)} < 0 \text{ stability}. \quad (7.7)$$

Metastability, in the sense defined above, occurs when

$$\epsilon^{(2)} < 0; \Delta H^{(2)} > 0 \text{ metastability}. \quad (7.8)$$

Obviously, no ordered compounds exist if both the chemical and the elastic energies are positive, i.e.,

$$\epsilon^{(2)} > 0; \Delta H^{(2)} > 0 \text{ no ordering}. \quad (7.9)$$

Figure 11(a) shows graphically the stability regimes of Eqs. (7.7) and (7.8). Since strain energy [$G(x)$ of Eq. (3.15)] is non-negative, we always have $\Delta H^{(2)} \geq \epsilon^{(2)}$. Hence, the half plane below the $\Delta H^{(2)} = \epsilon^{(2)}$ line is forbidden. Using $\Delta H^{(2)} = \Omega/4 + \epsilon^{(2)}$, we also give these regions in the $(\Omega, \epsilon^{(2)})$ plane [Fig. 11(b)] and the $(\Omega, \Delta H^{(2)})$ plane [Fig. 11(c)].

This analysis suggests that metastable long-range ordered compounds can exist within the miscibility gap if the constituents are sufficiently lattice-mismatched [to give $G(x) \gg 0$], provided the chemical interactions are sufficiently attractive. This is likely to be the case for systems such as Cu-Ag, for which we have recently predicted⁴² metastability at low temperatures. This highlights the difference between the ϵ - G approach and the ϵ -only approach of Kikuchi *et al.*:¹⁸ these authors were forced to assume $\epsilon > 0$ for Cu-Ag (in contrast with the common fact that Cu and Ag attract each other, forming a stable diatomic molecule, and with the fact that first-principles

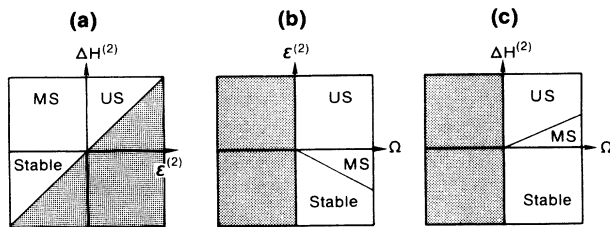


FIG. 11. Regions of stability, metastability (MS) and instability (US) of ordered compounds in the pair approximation (see Sec. VII C). Shaded areas denote regions of the parameters in which no phases exist.

self-consistent calculations⁴² reveal $\epsilon^{(n)} < 0$ for $\text{Cu}_n\text{Ag}_{4-n}$, since in the absence of $G(x)$, fitting the observed phase-separation behavior of Cu-Ag requires assuming a ferromagnetic repulsion. In contrast, the present approach correctly describes the phase separation behavior⁴² without resorting to an unmotivated assumption of $\epsilon > 0$. Furthermore, the use of a physically correct $\epsilon^{(n)} < 0$ (but $G(x) \gg 0$) provides also a qualitatively different prediction as to the existence of long-range ordered phases at low temperature.

This analysis has an important implication on lattice mismatched pseudobinary alloys of $AC+BC$. If the system has a sizeable lattice mismatch $\Delta a = |a_{AC} - a_{BC}|$, the elastic energy is large, yielding positive mixing enthalpies $\Delta H(x, T)$ and eventually a miscibility gap. This is the case for most isovalent semiconductor alloys,³⁶⁻³⁷ e.g., GaAs-GaSb. However, a large Δa also implies that the common sublattice C distorts (leading to near-ideal R_{AC} and R_{BC} bond lengths). Such distortions have been observed experimentally^{29,52} and calculated theoretically^{22,53} for many isovalent semiconductor alloys. These relaxations of the common sublattice constitute in our scheme a part of $\epsilon^{(n)}$ (see Sec. III. A), and contribute to its becoming negative. Hence, one can expect that lattice-mismatch pseudobinary semiconductor alloys satisfy condition (7.8) and should exhibit metastable long-range ordering inside the miscibility gap. This was indeed observed recently²⁴ for GaAs-GaSb, exhibiting chalcopyrite-like Ga_2AsSb ordered structures within the miscibility gap.

Whereas ϵ -only Ising models need to resort to rather artificial assumptions on the ratio of second- to first-neighbor interaction energies⁵⁴ to explain metastable solutions, the present approach shows such effects to simply result from the interplay between elastic and chemical effects. Indeed, the existence of concomitant atomic ordering and decomposition has been demonstrated to exist both in metallurgical systems⁵⁵ (Cu-Ti, Ni-Al, Cu-Ni-Sn, and Ni-Ti) and in semiconductor alloys (GaAs-GaSb).²⁴

VIII. SUMMARY

We have shown that when molar volumes at fixed composition do not depend on the state of order the equilibrium energy of the alloy $\Delta E(\sigma)$ can be expressed [Eq. (3.9)] as a sum over configurations n of volume and the composition independent (chemical) energies $\epsilon^{(n)}$ plus a configuration-independent (elastic) energy term $G(x)$. We show that both contributions are significant and essential. Both can be approximated either from experimental or from first-principles calculations on ordered compounds. This is illustrated for the $\text{Cu}_{1-x}\text{Au}_x$ alloy system for which we demonstrate that using structural and elastic data on the ordered phases $\text{Cu}_n\text{Au}_{4-n}$ suffices in our approach to predict order-disorder transition temperatures.

We have compared the traditional (ϵ -only) Ising configurational approach, on which we build, with the present one (ϵ - G) which incorporates both chemical (ϵ) and elastic (G) effects. We find the following elastic energy induced effects.

(i) Elastic energies $G(x)$ act to *narrow* the single-phase existence regions (Fig. 4), (hence *stabilize* ordered compounds) and to *broaden* the two-phase regions in the phase diagram.

(ii) Whereas the ϵ -only method leads to substantial overestimation of mixing enthalpies, the present approach leads to physically correct enthalpies (Fig. 5).

(iii) The incorporation of elastic effects acts to remove much of the ground state degeneracies characteristic of the ϵ -only Ising Hamiltonian (Fig. 6). This leads to a significant increase of the triple-point temperature relative to the ϵ -only pure Ising model (Fig. 7). (Indeed the pure Ising model, when applied to Cu-Au, yielded⁵⁰ a lower triple-point temperature relative to experiments).

(iv) Elastic effects lead to the possibility of metastable long-range ordered compounds even though their formation enthalpy $\Delta H^{(n)}$ is positive (Fig. 9). This is possible if the chemical energies $\epsilon^{(n)}$ are negative, but the positive elastic energy $G(x)$ overwhelms it. No such solutions exist in pure configurational pairwise Ising models. Such metastable solutions are likely to be pertinent in describing recently observed ordering both in metallurgy and in semiconductor alloys.

(v) The inclusion of elastic effects makes it possible to find stable, long-range order as well as miscibility gaps in *the same phase diagram*.²²⁻²⁴ This was predicted theoretically in Refs. 22 and 23 and subsequently observed experimentally.²⁴

(vi) Specialization of our general ϵ - G approach to the case of semiconductor alloys (where Vegard rules generally apply and where formation enthalpies are small) produces excellent agreement with the observed high-temperature alloy mixing enthalpies.

The ease of incorporation of the new elastic term $G(x)$ into conventional configurational Ising models promises to make the present ϵ - G approach a generally applicable method for realistic descriptions of alloy phase diagrams.

ACKNOWLEDGMENTS

This work was supported by the Solar Energy Research Institute SERI and by the Office of Energy Research (Office of Basic Energy Science, Division of Materials Science), U.S. Department of Energy, through Grant No. De-AC02-77CH00178.

APPENDIX A: DERIVATION OF THE ELASTIC ENERGY $G(x)$

Our central assumption here is that the equilibrium volumes $V(\sigma, x)$ have but a weak dependence on the state of order σ , and hence can be approximated by some $V(x)$ for which we will solve. In this Appendix we prove Eqs. (3.7)–(3.11) of the text under this assumption.

The results of Eqs. (3.7)–(3.11) are easy to prove when the different ordered arrangements have different concentrations X_n , that is

$$\text{if } n \neq n' \text{ then } X_n \neq X_{n'} . \quad (\text{A1})$$

At the end of this Appendix [Eqs. (A34)–(A38)] we discuss the particular case when $X_n = X_{n'}$. When Eq. (A1)

holds, the volume-dependent energy of the ordered arrangement n can be written as

$$\Delta E(n, V) = \sum_k X_n^k Y_k(V) , \quad (\text{A2})$$

where there are as many powers k of the concentration X_n , as there are ordered arrangements n . The functions $Y_k(V)$ are obtained from Eq. (A2) by inverting the matrix X_n^k . Then

$$\begin{aligned} \Delta E(\sigma, V) &= \sum_n \xi_n(\sigma) \Delta E(n, V) = \sum_k Y_k(V) \sum_n \xi_n(\sigma) X_n^k \\ &= \sum_k Y_k(V) \sum_n \xi_n(\sigma) [x + (X_n - x)]^k \\ &= \sum_k Y_k(V) \sum_l \binom{k}{l} x^{k-l} \sum_n \xi_n(\sigma) (X_n - x)^l , \end{aligned} \quad (\text{A3})$$

where the frequencies ξ_n are such that

$$x = \sum_n \xi_n(\sigma) X_n , \quad (\text{A4})$$

$$1 = \sum_n \xi_n(\sigma) . \quad (\text{A5})$$

Define the centered moments

$$\mu_l(\sigma, x) = \sum_n \xi_n(\sigma) (X_n - x)^l , \quad (\text{A6})$$

$$\mu_0 = 1, \quad \mu_1 = 0 . \quad (\text{A7})$$

Thus

$$\Delta E(\sigma, V) = \sum_l \mu_l(\sigma, x) \sum_k Y_k(V) \binom{k}{l} x^{k-l} . \quad (\text{A8})$$

The sums over n , k , and l in Eqs. (A3), (A6), and (A8) all have a finite number of terms: The sum on n is limited to the set of ordered arrangements being considered; the sum over k has the same extent [otherwise Eq. (A2) would not define $Y_k(V)$ unambiguously]. Finally, the sum on l is limited by the factor $\binom{k}{l}$ which is zero if $l < 0$ or $l > k$. Therefore, interchanging the order of the summations, as done in Eqs. (A3) and (A8) is permissible.

At given state of order σ , the equilibrium volume is the solution of

$$\frac{d\Delta E}{dV} = 0 = \sum_l \mu_l(\sigma, x) a_l(x, V) , \quad (\text{A9})$$

where

$$a_l(x, V) = \sum_k \frac{dY_k}{dV} \binom{k}{l} x^{k-l} . \quad (\text{A10})$$

The solution $V(\sigma, x)$ of Eq. (A9) can in general depend on the state of order σ . Under our assumption that the solution depends only on x , and is independent of σ (see discussion and justification in Sec. III B) Eq. (A9) can be rewritten as

$$\sum_l \mu_l(\sigma, x) a_l[x, V(x)] = 0 , \quad (\text{A11})$$

where we are stressing that the functions a_l depend only on x . Then we consider the set \sum_x of states of order σ satisfying Eq. (A4). We first observe that \sum_x is rich enough to allow independent variations of the moments μ_l with $l \geq 2$. Indeed, for any arbitrarily chosen set of values of μ_l (but with μ_0 and μ_1 satisfying Eqs. A4 and A5), the frequencies $\xi_n(\sigma)$ can be determined by inverting Eq. (A6). This inversion is always feasible, as long as Eq. (A1) is satisfied because the finite square matrix

$$\begin{pmatrix} 1 & 1 & 1 & \dots \\ (X_1-x) & (X_2-x) & (X_3-x) & \\ (X_1-x)^2 & (X_2-x)^2 & (X_3-x)^2 & \\ \vdots & & & \end{pmatrix}$$

is not singular. In fact, by combining rows of this matrix one readily sees that its determinant is equal to the determinant of

$$\begin{pmatrix} 1 & 1 & 1 & \dots \\ X_1 & X_2 & X_3 & \\ X_1^2 & X_2^2 & X_3^2 & \\ \vdots & & & \end{pmatrix},$$

a matrix which is clearly nonsingular. Some arbitrarily chosen sets of μ_l will lead to nonphysical frequencies for which

$$\xi_n(\sigma) < 0.$$

On the other hand, given a set $\mu_l^{(0)}$ of moments leading to positive frequencies $\xi_n^{(0)}$, there exists a neighborhood $[\mu_l^{(0)} - \Delta, \mu_l^{(0)} + \Delta]$ within which we can choose μ_l arbitrarily and independently, and for which the frequencies ξ_n are still positive. Since for given positive ξ_n 's one can always find many states of order σ [see discussion surrounding Eq. (2.5) of the main text], we conclude that, in the set \sum_x of states of order with composition x , we can find σ 's that permit arbitrary and independent variations of μ_l . Thus, we first write Eq. (A11) for a given set of physical $\mu_l^{(0)}$, i.e., moments that upon insertion into Eq. (A6) lead to positive frequencies. Next we take a neighboring σ in \sum_x whose moments are equal to $\mu_l^{(0)}$, except for $l=2$. Taking the difference between the two resulting Eqs. (A11) one finds that

$$a_l[x, V(x)] = 0 \quad \text{for } l \geq 2. \quad (\text{A12})$$

After arriving at the result above, Eqs. (A11) reduces to

$$a_0[x, V(x)] = 0. \quad (\text{A13})$$

Nothing can be said about a_1 , except that it is a function of x .

Equations (A12) and (A13) result from three assumptions: (i) that the internal energy for the alloy in the state of order σ can be written as a linear combination of the energy functions $\Delta E(n, V)$ of a few ordered arrangements; (ii) that the equilibrium volume is state-of-order independent, and only a function $V(x)$ of the concentra-

tion, so that Eq. (A9) can be rewritten as Eq. (A11); and (iii) that the ordered structures n are such that (A1) is satisfied, a necessary condition for the inversion of Eq. (A6). Later we show that assumption (iii) can be discarded if we place another restriction on the functions $\Delta E(n, V)$ of the ordered structures. These three assumptions are rather common in theoretical work on alloys. What is new here are Eqs. (A12) and (A13) and the consequences we now derive from them.

Eq. (A13) defines the function

$$V = V(x) \quad (\text{A14})$$

and its inverse

$$x = X(V). \quad (\text{A15})$$

Using V as independent variables, Eqs. (A12) and (A13) are written as

$$\sum_k \frac{dY_k}{dV} \begin{pmatrix} k \\ l \end{pmatrix} X(V)^{k-l} = 0 \quad (l \neq 1) \quad (\text{A16})$$

while for $l=1$ we write

$$\sum_k \frac{dY_k}{dV} \begin{pmatrix} k \\ l \end{pmatrix} X(V)^{k-1} = Z(V), \quad (\text{A17})$$

that is, a function of V named Z . Now, multiplying these Eqs. by powers of a variable t and adding

$$\sum_k \frac{dY_k(V)}{dV} [t + X(V)]^k = Z(V)t, \quad (\text{A18})$$

the many values of dY_k/dV can be found by taking derivatives with respect to t and setting

$$t = -X(V). \quad (\text{A19})$$

Thus

$$\frac{dY_0}{dV} = -Z(V)X(V), \quad (\text{A20})$$

$$\frac{dY_1}{dV} = Z(V), \quad (\text{A21})$$

$$\frac{dY_k}{dV} = 0 \quad (k \geq 2). \quad (\text{A22})$$

On integration

$$Y_0(V) = - \int^V Z(V')X(V')dV', \quad (\text{A23})$$

$$Y_1(V) = \int^V Z(V')dV', \quad (\text{A24})$$

and

$$Y_k = C_k \quad (k \geq 2), \quad (\text{A25})$$

which does not depend on V . We insert these results in Eq. (A2)

$$\Delta E(n, V) = - \int^V Z(V')X(V')dV' + X_n \int^V Z(V')dV' + \varepsilon^{(n)}, \quad (\text{A26})$$

where

$$\epsilon^{(n)} = \sum_{k \geq 2} X_n^k C_k. \quad (\text{A27})$$

Then, using Eqs. (A4) and (A5) we find

$$\begin{aligned} \Delta E(\sigma, V) = & - \int^V Z(V') X(V') dV' \\ & + x \int^V Z(V') dV' + \sum_n \xi_n(\sigma) \epsilon^{(n)}. \end{aligned} \quad (\text{A28})$$

The derivatives of Eq. (A28) are

$$\frac{d\Delta E}{dV} = [x - X(V)] Z(V), \quad (\text{A29})$$

$$\frac{d^2 E}{dV^2} = - \frac{dX}{dV} Z(V) + [x - X(V)] \frac{dZ}{dV}. \quad (\text{A30})$$

At equilibrium [Eq. (A15)], the first derivative is null, while the second derivative defines a bulk modulus also independent of the state of order

$$\frac{B(V)}{V} = - \frac{dX}{dV} Z(V). \quad (\text{A31})$$

Using Eq. (A31) in (A28), requiring that for the pure elements A and B (for which the state of order is denoted σ_A and σ_B , respectively) the energy is zero, so that we are actually dealing with the enthalpy of mixing, or

$$\Delta E(\sigma_A, V_A) = 0, \quad (\text{A32})$$

$$\Delta E(\sigma_B, V_B) = 0, \quad (\text{A33})$$

we arrive at Eqs. (3.7) and (3.8) of the text.

If two different ordered arrangements i and j had the same concentration, our basic assumption would require that they also had the same bulk modulus, thus their energy could differ just by a volume-independent constant

$$X_j = X_i \quad (\text{A34})$$

$$\Delta E(j, V) = \Delta E(i, V) + \Delta. \quad (\text{A35})$$

Thus in the sum

$$\Delta E(\sigma, V) = \sum_n \xi_n(\sigma) \Delta E(n, V) \quad (\text{A36})$$

the two terms

$$\xi_i \Delta E(i, V) + \xi_j \Delta E(j, V) = (\xi_i + \xi_j) \Delta E(i, V) + \xi_j \Delta \quad (\text{A37})$$

could be interpreted as a single ordered structure n with probability

$$\xi_n = \xi_i + \xi_j \quad (\text{A38})$$

and the last term in the right-hand side of Eq. (A37) would be added to the volume-independent last term of Eq. (B28).

APPENDIX B: RELATIONSHIPS BETWEEN $\epsilon^{(n)}$ AND ORDER-DISORDER TEMPERATURES, COMPOSITIONS, AND LATENT HEATS FOR BINARY fcc ALLOYS

For the binary fcc $A_{1-x}B_x$ alloy showing the $A_{4-n}B_n$ ground states (fcc for $n=0,4$, L_1 structure for $n=2$,

and L_2 structure for $n=1,3$), CVM calculations for nearest-neighbor interactions with up to four-atom interactions on a tetrahedron were performed for a large range of interaction parameters $\epsilon^{(n)}$. The solutions for this fcc spin- $\frac{1}{2}$ nearest-neighbor Ising model could be fit to give the following convenient relationships.

(A) The maximum temperatures T_n at which the ordered structure $A_{4-n}B_n$ exists in equilibrium with the disordered phase when both have the same concentration, can be given by

$$\begin{pmatrix} T_1 \\ T_2 \\ T_3 \end{pmatrix} = \begin{pmatrix} -453.32 & 208.92 & 11.80 \\ 201.34 & -421.11 & 201.34 \\ 11.80 & 208.92 & -453.32 \end{pmatrix} \begin{pmatrix} \epsilon^{(1)} \\ \epsilon^{(2)} \\ \epsilon^{(3)} \end{pmatrix}, \quad (\text{B1})$$

where $\epsilon^{(n)}$ is in kcal/mol, and T_n is in degrees Kelvin. This fit is exact in the pair-approximation ($\epsilon^{(1)} = \epsilon^{(3)} = \frac{3}{4}\epsilon^{(2)}$). Defining the non-pairwise interaction parameters¹⁷

$$\begin{aligned} \alpha &= \frac{4}{3} \frac{\epsilon^{(1)}}{\epsilon^{(2)}} - 1, \\ \beta &= \frac{4}{3} \frac{\epsilon^{(3)}}{\epsilon^{(2)}} - 1, \end{aligned} \quad (\text{B2})$$

we find that Eq. (A1) produces errors below 0.3% for α, β of the order of ± 0.1 . The errors are below 1.6% if α and β are of the order of ± 0.2 .

(B) The concentrations x_n at the maximum temperatures T_n are given by

$$\begin{pmatrix} x_1 \\ x_2 \\ x_3 \end{pmatrix} = \begin{pmatrix} 0.3902 \\ 0.5 \\ 0.6098 \end{pmatrix} + \begin{pmatrix} -0.1347 & -0.0320 \\ -0.0347 & 0.0347 \\ 0.0320 & 0.1347 \end{pmatrix} \begin{pmatrix} \epsilon^{(1)}/\epsilon^{(2)} \\ \epsilon^{(3)}/\epsilon^{(2)} \end{pmatrix}. \quad (\text{B3})$$

This again is exact for pair interactions ($\alpha = \beta = 0$); for α, β of the order of ± 0.1 , the errors in x_n are below 0.005, whereas for α, β of order ± 0.2 the errors are below 0.012. Note that Eqs. (A1) and (A3) show that a maximum temperature T_n need not always exist (e.g., for $\alpha = 0, \beta = -0.2$, the maximum T_3 at x_3 , disappears).¹⁷ A good way to find whether a maximum exists is to calculate the latent heat L_n .

(C) The latent heat L_n for transformation of phase n can be given as

$$\begin{pmatrix} L_1 \\ L_2 \\ L_3 \end{pmatrix} = \begin{pmatrix} -0.3161 & 0.2066 & -0.0307 \\ 0.2199 & -0.3937 & 0.2199 \\ -0.0307 & 0.2066 & -0.3161 \end{pmatrix} \begin{pmatrix} \epsilon^{(1)} \\ \epsilon^{(2)} \\ \epsilon^{(3)} \end{pmatrix}. \quad (\text{B4})$$

If $L_n < 0$, no maximum exists for the order-disorder transition for phase n . For example, for $\alpha = 0$, L_3 first becomes negative (indicating the disappearance of the maximum at x_3 , T_3) for $\beta = -0.23$, in very good agreement with the earlier results of Van Baal.¹⁷

Although the matrices of Eqs. (B1)–(B4) were calculated only for small ($\lesssim 0.2$) α and β values, we find that they represent good fits also for a larger range of values. For example, for $\alpha = \beta = -1$ ($\epsilon^{(1)} = \epsilon^{(3)} = 0$) one has by Eq.

(B4) $L_1 < 0$ and $L_3 < 0$, so only the phase $n=2$ has a maximum in the phase diagram. This maximum at $x=0.5$ is predicted by Eq. (B1) to occur at $T_2 = -421.11\varepsilon^{(2)}$. A direct CVM calculation gives $T_2 = -378.6\varepsilon^{(2)}$. Considering the large range of α and β involved, the error is reasonably small.

(D) To complete this short description of CVM results for fcc crystals we show how to relate the chemical energies $\varepsilon^{(n)}$ to the tetrahedron probabilities in the disordered state. In semiconductor alloys, one seldom knows the transition temperatures, but frequently determines how much the probabilities diverge from those $P_n^{(R)}$ of a completely random alloy

$$P_n^{(R)} = \binom{4}{n} (1-x)^{4-n} x^n. \quad (\text{B5})$$

We found that for high temperatures, and a very broad range of negative or positive $\varepsilon^{(n)}$, P_n , and $P_n^{(R)}$ could be related by the following:

(i) At concentration $x=0.25$,

$$\begin{pmatrix} \ln P_0/P_0^{(R)} \\ \ln P_1/P_1^{(R)} \\ \ln P_2/P_2^{(R)} \\ \ln P_3/P_3^{(R)} \\ \ln P_4/P_4^{(R)} \end{pmatrix} = \frac{1}{T} \begin{pmatrix} 177.6 & -5.5 & -43.4 \\ -216.7 & 40.7 & 36.8 \\ 82.1 & -132.4 & 53.2 \\ 318.9 & 230.0 & -245.8 \\ 745.4 & 373.1 & -105.4 \end{pmatrix} \begin{pmatrix} \varepsilon^{(1)} \\ \varepsilon^{(2)} \\ \varepsilon^{(3)} \end{pmatrix}. \quad (\text{B6})$$

(ii) At concentration $x=0.50$,

$$\begin{pmatrix} \ln P_0/P_0^{(R)} \\ \ln P_1/P_1^{(R)} \\ \ln P_2/P_2^{(R)} \\ \ln P_3/P_3^{(R)} \\ \ln P_4/P_4^{(R)} \end{pmatrix} = \frac{1}{T} \begin{pmatrix} 190.1 & 283.9 & -60.4 \\ -126.4 & 94.2 & 0.0 \\ 61.8 & -220.7 & 61.8 \\ 0.0 & 94.2 & -126.4 \\ -60.4 & 283.9 & 190.1 \end{pmatrix} \begin{pmatrix} \varepsilon^{(1)} \\ \varepsilon^{(2)} \\ \varepsilon^{(3)} \end{pmatrix}. \quad (\text{B7})$$

(iii) At concentration $x=0.75$ the result is the same as $x=0.25$, if one interchanges subscripts 1 and 3.

Eqs. (B6)–(B7), which resulted from a linearization of the CVM results for $(\varepsilon^{(1)}, \varepsilon^{(2)}, \varepsilon^{(3)}) = (\pm 6, \pm 8, \pm 6)$, are useful for a qualitative prediction of clustering in semiconductor alloys. They also clarify the facts that (i) clustering or anticlustering [$P_n(x) \neq P_n^{(R)}(x)$] manifests only the contribution of the chemical energies $\{\varepsilon^{(n)}\}$ (not strain energies); (ii) since relaxation of the *common* sublattice is part of $\varepsilon^{(n)}$ (see Sec. III A), and since ternary systems $A_x B_{1-x} C$ with a large AC - BC lattice mismatch exhibit substantial relaxations of the common sublattice, they are expected to show significant clustering, and (iii) these equations clarify the conditions (i.e., values of $\varepsilon^{(n)}$) which give no clustering, or anticlustering, i.e., $P_n(x) = P_n^{(R)}(x)$.

*Permanent address: Universidade de São Paulo, 05 508 São Paulo, Brazil.

†Permanent address: Laboratoire de Physique du Solide et Énergie Solaire (LPHSES), Centre National de la Recherche Scientifique, Parc de Sophia Antipolis, rue Bernard Gregory, 06560 Valbonne, France.

¹W. B. Pearson, *The Crystal Chemistry and Physics of Metal Alloys* (Wiley-Interscience, New York, 1972).

²L. S. Darken and R. W. Gurry, *Physical Chemistry of Metals*, (McGraw-Hill, New York, 1953).

³A. R. Miedema, R. Boom, and F. R. deBoer, *J. Less-Common Met.* **40**, 283 (1975).

⁴W. Hume-Rothery, R. E. Smallman, and C. W. Haworth, *Structure of Metals and Alloys*, 5th ed. (Institute of Metals, London, 1969).

⁵L. Pauling, *The Nature of the Chemical Bond* (Cornell University Press, Ithaca, New York, 1960).

⁶A. F. Wells, *Structural Inorganic Chemistry* (Clarendon, Oxford, 1975).

⁷E. Mooser and W. B. Pearson, *Acta. Crystallogr.* **12**, 1015 (1959).

⁸A. Zunger, *Phys. Rev. Lett.* **44**, 582 (1980); *Phys. Rev. B* **22**, 5839 (1980); J. St. John and A. N. Bloch, *Phys. Rev. Lett.* **33**, 1095 (1974); J. R. Chelikowsky and J. C. Phillips, *Phys. Rev. B* **17**, 2453 (1978).

⁹*Phase Stability of Metals and Alloys*, edited by P. Rudman, J. Stringer and R. I. Jaffee (McGraw-Hill, New York, 1967).

¹⁰E. Parthé, *Crystal Chemistry of Tetrahedral Structures* (Gordon and Breach, New York, 1964).

¹¹O. Kubaschewski in *Phase Stability of Metals and Alloys*, Ref. 9, p. 63 and Fig. 3.

¹²C. Domb, in *Phase Transition and Critical Phenomena*, edited by C. Domb and H. S. Green (Academic, London 1974), Vol. 3, pp. 357.

¹³D. De Fontaine, in *Solid State Physics*, edited by H. Ehrenreich, F. Seitz, and D. Turnbull (Academic, New York, 1979), Vol. 73. See the treatment of next-nearest-neighbor interactions in J. M. Sanchez and D. deFontain, *Phys. Rev. B* **21**, 216 (1980); **25**, 1759 (1983).

¹⁴D. M. Burley, in *Phase Transitions and Critical Phenomena*, edited by C. Domb and M. S. Green (Academic, London, 1972) Vol. 2, 329.

¹⁵J. Hijmans and J. De Boer, *Physica (Utrecht)* **21**, 471 (1955); **21**, 485 (1955); **21**, 499 (1955).

¹⁶(a) R. Hultgren, R. D. Desai, D. T. Hawkins, H. G. Gleiser and K. K. Kelley, *Selected Values of the Thermodynamic Properties of Binary Alloys* (American Society for Metals, Cleveland, 1973); for Cu-Au see (b) P. M. Hansen and K. Anderko, *Constitution of Binary Alloys*, 2nd ed. (McGraw-Hill, New York, 1958), pp. 198–203; (c) see also *Constitution of Binary Alloys, First Supplement* (McGraw-Hill, New York, 1965), pp. 87–88.

¹⁷C. M. van Baal, *Physica (Utrecht)* **64**, 571 (1973).

¹⁸R. Kikuchi, J. M. Sanchez, D. De Fontaine, and H. Yamachi, *Acta. Metall.* **28**, 651 (1980); R. Kikuchi, in *Noble Metal Alloys*, edited by T. B. Massalski, W. B. Pearson, L. H. Bennett, and Y. A. Chang (The Metallurgical Society, Warrendale, Pennsylvania, 1986), p. 63.

- ¹⁹D. F. Styer, M. K. Phani, and J. Lebowitz, *Phys. Rev. B* **34**, 3361 (1986).
- ²⁰K. Binder, *Phys. Rev. Lett.* **45**, 811 (1980).
- ²¹See, e.g., Ya. G. Sinai, *Theory of Phase Transitions: Rigorous Results* (Pergamon, Oxford, 1982).
- ²²G. P. Srivastava, J. L. Martins, and A. Zunger, *Phys. Rev. B* **31**, 2561 (1985).
- ²³A. A. Mbaye, L. G. Ferreira, and A. Zunger, *Phys. Rev. Lett.* **58**, 49 (1987).
- ²⁴H. R. Jen, M. J. Cherng, and G. B. Stringfellow, *Appl. Phys. Lett.* **48**, 1603 (1986); H. Nakayama and H. Fujita, in *Gallium Arsenide and Related Compounds, 1985*, Inst. Phys. Conf. Ser. No. 79, edited by M. Fujimoto (IOP London, 1986) p. 289; M. A. Shahid, S. Mahajan, D. E. Laughlin and H. M. Cox, *Phys. Rev. Lett.* **58**, 2567 (1987); T. S. Kuan, W. I. Wang, and E. L. Wilkie, *Appl. Phys. Lett.* **51**, 51 (1987).
- ²⁵(a) A. B. Chen and A. Sher, in *Microscopic Identification of Electronic Defects in Semiconductors*, Vol. 46 of Mater. Res. Soc. Symp. Proc., edited by N. M. Johnson, S. G. Bishop and G. D. Watkins (MRS, Pittsburgh, 1985); (b) A. Sher, A. B. Chen, and M. Van Schilfgaarde, *J. Vac. Sci. Technol. A* **4**, 1965 (1986).
- ²⁶M. A. Krivoglaz, *The Theory of X-Rays and Thermal Neutron Scattering of Real Crystals* (Fizmatgiz, Moscow, 1967) (in Russian).
- ²⁷C. Sigli and J. M. Sanchez, *CALPHAP* **8**, 221 (1981).
- ²⁸J. W. D. Connolly and A. B. Williams, *Phys. Rev. B* **27**, 5169 (1983); K. Terakura, T. Oguchi, T. Mohri, and K. Watanabe, *Phys. Rev. B* **35**, 2169 (1987).
- ²⁹M. T. Czyzyk, M. Podgorny, A. Balzarotti, P. Letardi, N. Motta, A. Kisiel, and M. Zimnal-Strnawska, *Z. Phys. B* **62**, 153 (1986).
- ³⁰V. T. Bublik and V. N. Leikin, *Phys. Status Solidi A* **46**, 365 (1978).
- ³¹P. A. Fedders and M. W. Muller, *J. Phys. Chem. Solids* **45**, 685 (1984).
- ³²L. Vegard, *Z. Phys.* **5**, 17 (1921).
- ³³L. G. Ferreira, A. A. Mbaye, and A. Zunger, *Phys. Rev. B* **35**, 6475 (1987). See also Ref. 42 below.
- ³⁴*Landolt-Börnstein*, New Series, edited by K.-H. Hellwege (Springer-Verlag, Berlin 1971) Vol. 6; Vol. 11 (1979).
- ³⁵We use the phrase "stable (unstable) ordered compound" to indicate whether $\Delta H^{(n)}$ is negative (positive). By this we imply stability or instability towards dissociating of these ordered compounds, without any implication on the disordered phase. Stability or instability with respect to a *miscibility gap* is decided, in turn, by the derivatives of the free energy with respect to composition, and is treated separately.
- ³⁶M. B. Panish and M. Ilegems, *Proc. Solid State Chem.* **7**, 39 (1972).
- ³⁷G. B. Stringfellow, *J. Cryst. Growth* **27**, 21 (1974); **58**, 194 (1982); *J. Appl. Phys.* **54**, 404 (1983).
- ³⁸R. F. Brebrick, C. H. Su, and P. K. Liao in *Semiconductors and Semimetals*, edited by R. K. Willardson and A. C. Beer (Academic, New York, 1983), Vol. 19, p. 171.
- ³⁹E. A. Guggenheim, *Mixtures* (Clarendon, Oxford, 1959).
- ⁴⁰A. G. Khachaturyan, *Theory of Structural Transformations in Solids*, (Wiley, New York, 1983).
- ⁴¹R. Kikuchi, *J. Chem. Phys.* **60**, 1071 (1974); *Phys. Rev.* **81**, 988 (1951). See also Ref. 13 for a review.
- ⁴²S. H. Wei, A. A. Mbaye, L. G. Ferreira, and A. Zunger, *Phys. Rev. B* **36**, 4163 (1987).
- ⁴³H. L. Yakel, *J. Appl. Phys.* **33**, 2439 (1962); P. A. Flinn, G. M. McManus, and J. A. Rayne, *J. Phys. Chem. Solids* **15**, 189 (1960).
- ⁴⁴P. Wright and K. F. Goddard, *Acta Metall.* **7**, 757 (1959).
- ⁴⁵In the CVM, it is always more convenient to work with the independent variables (μ, T) instead of (x, T) . One must exercise care in including the $G(x)$ term in CVM programs. If one follows Kikuchi's derivation (Ref. 41) of the formulas leading to the natural iterations in CVM, one readily finds that, by including $G(x)$ in the Hamiltonian, all one has to do is to work with the effective chemical interactions $\epsilon^{(n)} + G(x) + (X_n - x)dG/dx$ instead of simply $\epsilon^{(n)}$. In this case, the natural iterations converge very well, and the meaning of the variables (Ref. 41) λ, μ remain as they were.
- ⁴⁶In general, the sum over n in Eq. (2.6) should extend over the 2^N arrangements of the N atoms in the crystal. If one considers instead periodic *supercells* with M atoms per supercell, the sum extends over 2^M . The smallest value of M which can be expected to give reasonable results would then correspond to a cell containing all "strong" interactions. In practice this can be determined by examining if the energy for any ordered structure with a *larger* supercell (M') can be expressed as a linear combination [Eq. (2.6)] of the energies of a smaller (M) supercells. For fcc systems, for example, this linearity problem can be decided by comparing the energy of the CuPt structure (having A_3B and AB_3 tetrahedra in the same unit cell) with the average of the energies of A_3B and AB_3 determined separately from the smaller supercells of the $L1_2$ (Cu₃Au-type) structure. Such comparisons (Ref. 42) for the Cu-Au system indicate that $M=4$ (i.e., the use of A_4 , A_3B , A_2B_2 , AB_3 and supercells) is sufficient. (This was also demonstrated in Ref. 28). We hence use in Eq. (4.13) $M=4$ and sum in Eq. (4.14) over $2^4=16$ clusters. This choice of tetrahedra A_4B_{4-n} centered around as the basic repeat unit seems also particularly reasonable for fourfold-coordinated covalent semiconductors where all bonds between an anion (C) and its nearest cations (A, B) are included in the basic unit. Note that if the linearity holds for $M > 4$, then the prefactor in Eq. (4.14) is still converged to $\frac{3}{4}$, whereas for $M=2$ (for which linearity does not hold) the prefactor is $\frac{1}{2}$.
- ⁴⁷D. M. Wood, S. H. Wei, and A. Zunger, *Phys. Rev. Lett.* **58**, 1123 (1987).
- ⁴⁸S. H. Wei and A. Zunger, *Phys. Rev. Lett.* **56**, 2391 (1986).
- ⁴⁹M. L. Cohen, *Phys. Rev. B* **32**, 7988 (1985).
- ⁵⁰K. Binder, J. L. Lebowitz, M. K. Phani, and M. H. Kalos, *Acta Metall.* **29**, 1655 (1981). See more recent results on the triple point by A. Finel and F. Ducastelle, *Europhys. Lett.* **1**, 135 (1986), as well as H. T. Diep, A. Ghazali, B. Berge, and P. Lallemand, *Europhys. Lett.* **2**, 603 (1986).
- ⁵¹In the Monte Carlo method, the spin-flip energy is calculated by counting the tetrahedra. To that term one then adds $G(x^1) - G(x) - \mu(x^1 - x)$, where x and x^1 are the concentrations before and after the spin flip, and where μ is the chemical potential, considered as an independent variable.
- ⁵²J. C. Mikkelsen and J. B. Boyce, *Phys. Rev. Lett.* **49**, 1412 (1982); *Phys. Rev. B* **38**, 7130 (1983).
- ⁵³J. L. Martins and A. Zunger, *Phys. Rev. B* **30**, 6216 (1984).
- ⁵⁴S. M. Allen and J. W. Cahn, *Acta Metall.* **24**, 425 (1976); D. E. Laughlin and J. W. Cahn, *ibid.* **23**, 3291 (1975).
- ⁵⁵D. E. Laughlin, K. B. Alexander and L. L. Lee, in *Decomposition of Alloys: The Early Stages*, edited by P. Haasen, V. Gerold, R. Wagner, and M. F. Ashby (Pergamon, Oxford, 1984); W. A. Soffa and D. E. Laughlin, *Proceedings of an International Conference on Solid-Solid Phase Transformations* (AIME, Warrendale, PA, 1981), pp. 159.

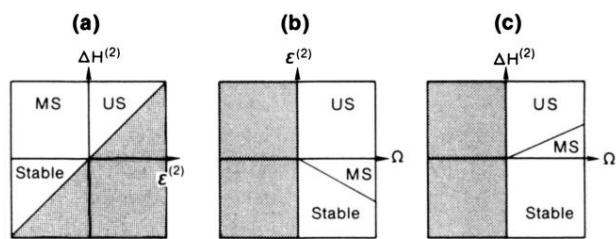


FIG. 11. Regions of stability, metastability (MS) and instability (US) of ordered compounds in the pair approximation (see Sec. VII C). Shaded areas denote regions of the parameters in which no phases exist.

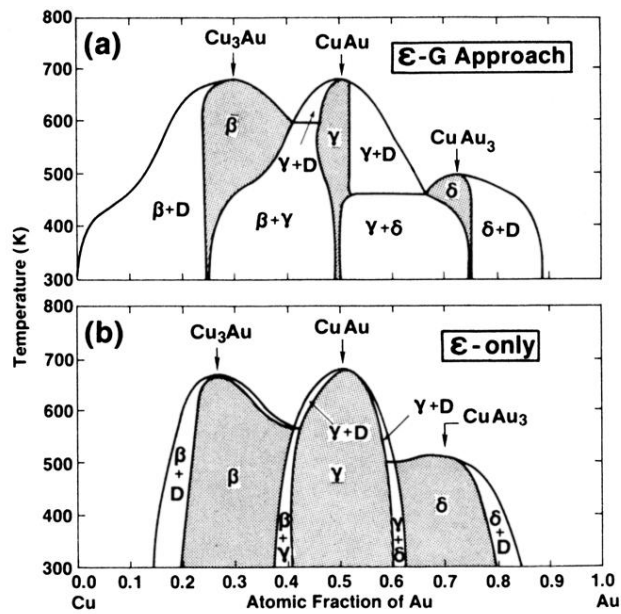


FIG. 4. CVM phase diagram for Cu-Au in the nearest-neighbor tetrahedron approximation: (a) in the ϵ - G approach, i.e., including both elastic and chemical interactions, using $\epsilon^{(n)}$ of Eq. (4.6) and $G(x)$ of Fig. 3 (constant Ω); (b) in the ϵ -only approach, i.e., neglecting the elastic interaction. Note that the single phase (two-phase) regions are much narrower (broader) in (a) relative to (b).